European Journal of Operational Research xxx (xxxx) xxx

Contents lists available at ScienceDirect

European Journal of Operational Research

journal homepage: www.elsevier.com/locate/ejor

Decision Support

Incentive rate determination in viral marketing

Ali Tavasoli[a,*], Heman Shakeri[b], Ehsan Ardjmand[c], William A. Young II[c]

[a] Department of Mechanical Engineering, Payame Noor University, Tehran, Iran
[b] School of Data Science, University of Virginia, Charlottesville, VA, USA
[c] Department of Analytics and Information Systems, College of Business, Ohio University, OH, 45701, USA

ARTICLE INFO

Article history:
Received 11 March 2020
Accepted 22 July 2020
Available online xxx

Keywords:
OR in marketing
Incentive rate determination
Dynamical systems over networks
Nonlinear programming
Epidemic spread

ABSTRACT

In viral marketing campaigns, incentivized consumers can act as sales agents by sharing information. In this study, we investigate the problem of incentive rate determination over a network of consumers to maximize the profit of a single good by a monopolist. For this purpose, we develop an epidemic spreading model to explore the dynamics of a viral marketing campaign under network externalities and incentivized individuals. We will examine two cases of homogeneous and heterogeneous incentive rates. In each case, we derive an N-intertwined dynamics model and obtain the existence and stability conditions of a trade-free or an endemic equilibrium. By treating the incentive as a control parameter, we investigate the problem of maximizing the monopolist's profit by formulating two nonlinear programming models. In the case of homogeneous incentive rates, results show that the optimal incentive is determined by devising a balance between the consumers' states in the Markov process. In the heterogeneous case, it is observed that despite the existence of a strong correlation with different centrality measures, the optimal incentive allocation cannot be solely determined by centrality measures.

1. Introduction

Social interactions influence product adoptions and purchasing behavior of consumers (Ameri, Honka, & Xie, 2019; Goel, Anderson, Hofman, & Watts, 2015). It has been shown that peer influence can increase the likelihood of buying a product by more than 60% (Bapna & Umyarov, 2015) and encourage further customer referrals (Biyalogorsky, Gerstner, & Libai, 2001). According to one estimation, between 20% and 50% of all purchasing choices are encouraged by personal recommendations (Meyners, Barrot, Becker, & Bodapati, 2017). Businesses have leveraged the power of influence because there is a synergy between the growing number of products and services that can be purchased online and the number of users relying on social media as their primary source of product and service information and reviews. The essence of these types of marketing strategies, which is collectively called viral marketing, is to promote a discussion around a product or service by disseminating information through a network of customers' social interactions (Bampo, Ewing, Mather, Stewart, & Wallace, 2008; Hinz, Skiera, Barrot, & Becker, 2011). Viral marketing campaigns benefit from targeted communication, speed of diffusion, and a high degree of integrity (Bampo et al., 2008).

The success of a viral marketing campaign is commonly measured by the number of potential consumers it reaches and the amount of sales it generates (Ajorlou, Jadbabaie, & Kakhbod, 2016; Hu, Milner, & Wu, 2015). Thus, a successful viral marketing campaign depends on the ability to share information effectively. The ability to share information in a network depends on the content being shared (Berger & Milkman, 2010), the structure of the social network (Bampo et al., 2008), the consumers' characteristics (Pescher, Reichhart, & Spann, 2014), and seeding strategy (Hinz et al., 2011). For instance, it has been shown that compared to small-world networks, scale-free networks offer a more effective medium for spreading processes of viral marketing campaigns. Furthermore, it is observed that a larger number of initializing seeds (although at the expense of profitability) increases the number of individuals reached in a diffusion process.

Marketers usually engineer the dispersion of information in a social network through carefully selecting a set of initial consumers, referred to as seeds, to set the viral marketing campaign in motion or to incentivize information sharing by providing intrinsic or extrinsic rewards (Van der Lans, Van Bruggen, Eliashberg, & Wierenga, 2010). In network science literature, controlling the diffusion of information in a network is usually studied under the topic of influence maximization (Hinz et al., 2011; Kempe, Kleinberg, & Tardos, 2003; Mandel & Venel, 2020; Tanınmış, Aras, & Altınel, 2019), where the goal is to maximize the number of potential consumers that are exposed to a viral marketing or information

* Corresponding author.
E-mail addresses: a.tavasoli@albpnu.ac.ir (A. Tavasoli), hs9hd@virginia.edu (H. Shakeri), ardjmand@ohio.edu (E. Ardjmand), youngw1@ohio.edu (W.A. Young II).

https://doi.org/10.1016/j.ejor.2020.07.046
0377-2217/

propagation campaign. A large number of studies in this field are dedicated to identifying a subset of individuals whose network influence can maximize the outreach of information. This problem, usually known as target set selection (TSS), is dependent on the process by which information is diffused in a network (Raghavan & Zhang, 2019) and is closely related to pricing problems in networks where the objective is to maximize profitability under social influence and network externalities.

Information propagation over complex networks is generally a stochastic phenomenon that is dynamically considered as an epidemic spreading process. The stochastic nature complicates the study of the dynamic behavior of epidemic spreading processes on network graphs, even for simple scenarios (Kiss, Miller, Simon et al., 2017; Newman, 2018). On the other hand, real networks usually consist of a large body of agents, which renders the problem of analyzing information diffusion intractable (Sahneh, Chowdhury, Brase, & Scoglio, 2014; Van Mieghem, Omic, & Kooij, 2009a). To simplify the problem, various works consider a deterministic approximation of the stochastic dynamics using the mean field epidemic models (Sahneh, Scoglio, & Van Mieghem, 2013b; Van Mieghem et al., 2009a), where the size of the problem is reduced dramatically, although at the expense of exactness. The mean approximation strategy has proven successful in deducing significant structural results, and analyzing information propagation dynamics over complex networks (Kiss et al., 2017; Newman, 2018; Nowzari, Preciado, & Pappas, 2016).

Most of the influence maximization literature, and specifically TSS, is structured around the objective of maximizing the number of individuals exposed to information or the survival duration of a viral process (Stewart, Ewing, & Mather, 2004). In a marketing setting, in addition to the sheer number of individuals, the amount of profit generated by a campaign (or conversion rate) is also important. In this regard, profit seems to be a more natural objective function for controlling the dynamics of a viral marketing campaign. Furthermore, there are very few studies that investigate the incentivizing strategies in which an individual is rewarded based on the amount of sales she generates through sharing information (Ajorlou & Jadbabaie, 2019). In this setting, individuals act as sales agents who can benefit from an incentive, usually materialized in the form of monetary payments or commission rates, if they can utilize their influence over their direct neighbors on a social network and generate sales.

This study contributes to the body of literature involving the influence maximization in viral marketing. In particular, the research presented in this article explores maximizing profit as the objective function while utilizing an incentive-based influence schema. For this problem, henceforth referred to as incentive rate determination (IRD), we assumed that the viral marketing campaign is conducted by a monopolist that is interested in promoting a single good. We consider an incentivizing schema similar to the one proposed by Lobel, Sadler, and Varshney (2016), in which a consumer receives a link to share with their connections upon buying the product. Every purchase made through the link generates a monetary reward for the customer sharing it. Additionally, the optimization schema developed incorporates an incentive rate as a control parameter and utilizes dynamical systems methodologies to extract results related to the dynamic epidemic phenomena that take place over social networks.

IRD problem does not assume a constrained set of individuals to start off a diffusion process. This means each individual is rewarded upon generating sales. In addition to the information diffusion process, IRD is dependent on the behavioral characteristics of individuals when offered an incentive to act as sales agents. Naturally, one expects to observe an increasing likelihood of willingness to share information by individuals as the sales commission increases. On the other hand, increasing sales commission can be detrimental to the profit margins of a business that aims at maximizing its marketing campaign outreach. Similarly, decreasing sales commissions can hurt the profit through a reduced size of consumers' population exposed to the marketing campaign. Thus, there is a tradeoff between influence maximization through incentivizing potential consumers and optimizing profit.

In this study, a monopolist is interested in targeting a network of consumers, represented as a graph. The nodes and links of the graph represent the individual consumers and their relations accordingly. Furthermore, it is assumed that each individual can be either a buyer ("B"), an owner ("O"), or a seller ("S"). A buyer is a potential consumer who may purchase the advertised merchandise in the marketing campaign. An owner is a consumer who owns the product but does not share information and, thus, does not function as a sales agent. A seller is a product owner that shares information actively and may generate sales by introducing the product or service to her contacts within the social network. The monopolist generates revenue every time a potential buyer turns into an owner or a seller. In this regard, sellers take the vital function of promoting the product and facilitate the process of the buyer to owner/seller conversion. Thus, the monopolist may want to encourage a larger body of the consumers to become sellers by monetarily incentivizing them. A more generous incentive schema can create more sellers. However, over-incentivization can hurt the monopolist's profit. On the other hand, under-incentivization can discourage consumers from promoting the product and restrict the sales and hence, the profit. Thus, the monopolist has to strike a balance between the extra sales generated by reaching more consumers and the cost of outreach through incentivization.

This study takes advantage of a continuous-time Markov process to model the transition of consumers between different roles of buyers, owners, and sellers based on the individuals' interactions in the network, and the subsequent monopolist's profit. For this purpose, an N-intertwined model (Van Mieghem et al., 2009a) that is the mean field approximation of the considered continuous-time Markov process, is utilized. Compared to the exact Markov model, the N-intertwined model makes only one approximation of a mean-field kind that results in upper bounding the exact model for finite network size N (Mieghem, 2011). Two general cases of homogeneous and heterogeneous incentive rates are investigated. In each case, the optimum incentive rate (i.e., the rate which maximizes the profit) and the conditions under which the trade-free and endemic equilibrium can exist and the corresponding stability conditions are identified. The trade-free equilibrium is the trivial equilibrium point where the individuals will steadily remain in Buyer state after a transient time and there will be no trading, while in endemic equilibrium state transitions between the states B, O and S occur continuously. By deriving explicit expression for the reproduction number[1] in each case, we show that the two determining elements of the sales propagation process are the amount of the incentive given and the spectral radius of the network (i.e., the largest eigenvalue of network's adjacency matrix). This study sheds light on some characteristics of optimal incentivization policies under homogenous and heterogenous incentive quantities, which can help with executing effective viral marketing campaigns.

The remaining sections of the paper are organized in the following manner. Section 2 briefly reviews the existing literature. Section 3 demonstrates the developed model. In

[1] The basic reproduction number, a key concept in epidemiology, is defined as the expected number of new cases of infection caused by a typical infected individual in a population of susceptibles (Fall, Iggidr, Sallet, & Tewa, 2007). In the context of this study, the reproduction number translates into the expected number of individuals that become an owner or seller of the product as a result of neighboring a consumer that owns or promotes the product.

Section 4, we study the existence and stability conditions of trade-free and endemic equilibrium states in the homogeneous incentive rate case. In Section 5, we introduce the profit function and investigate its properties. In addition, we define a nonlinear programming model that determines the optimal incentive that results in the maximum profit for homogeneous rates. The next two sections examine the case of heterogeneous incentives. In Section 6, we introduce the heterogeneous IRD model, and characterize the trade-free and endemic equilibria properties. In Section 7, we examine the problem of profit maximization in heterogeneous cases. In Section 8, we provide some managerial implications. Finally, Section 9 concludes the study.

2. Literature review

The effect of network externalities and seeding policies on viral marketing strategies and TSS problems are studied extensively in the literature (Ajorlou & Jadbabaie, 2019; Arthur, Motwani, Sharma, & Xu, 2009; Bloch & Quérou, 2013; Candogan, Bimpikis, & Ozdaglar, 2012; Chen et al., 2011; Cohen & Harsha, 2019; Hartline, Mirrokni, & Sundararajan, 2008). As a result, multiple influence maximization schemas are suggested. For example, inspired by the policy of influence maximization (Domingos & Richardson, 2001; Kempe et al., 2003), influence-and-exploit seeding strategies initially influence the population by providing free products to a chosen set of buyers. Then revenue is realized from the remaining potential consumers using a greedy pricing strategy (Arthur et al., 2009; Hartline et al., 2008). Other research found in the literature emphasizes the role of network centrality measures. These studies recognize that optimal monopoly pricing in social networks is mainly affected by the set of central or influential agents (Bloch & Quérou, 2013; Candogan et al., 2012; Cohen & Harsha, 2019; Hinz et al., 2011). These influential agents may be offered either favorable prices, whenever they are targeted to influence other agents or unfavorable prices, whenever they are targeted for sale (Carroni, Pin, & Righi, 2019). The optimal prices in social networks can be time-varying. Indeed, a dynamic pricing strategy (Ajorlou et al., 2016) reveals the conditions when the optimal prices are neither monotone nor reach a steady state; instead, they fluctuate.

While similar in nature and objectives, IRD differs from TSS in the allocation of resources (i.e., incentive) to individuals and the structure of its incentive system. In IRD, one concern is how to distribute the available incentive throughout a given contact network so that the profit is maximized. This issue is best answered in the framework of optimal distribution of resources (Preciado, Zargham, Enyioha, Jadbabaie, & Pappas, 2013; 2014; Shakeri, Sahneh, Scoglio, Poggi-Corradini, & Preciado, 2015; Watkins, Nowzari, & Pappas, 2017; 2018). Optimization strategies are proven more effective, in particular, when individuals in the network show different levels of reaction to an epidemic or the spread of information. To be solved more efficiently, these problems are usually reformulated as convex, semidefinite, or quasiconvex optimization problems known as geometric programs (Boyd, Kim, Vandenberghe, & Hassibi, 2007). The solutions of the optimization problems yield nontrivial patterns that cannot, in general, be described using simple heuristics based on common network centrality measures.

Some related studies are concerned with a general representation of contact networks when investigating the general epidemic phenomena and optimal resource allocation problem. In these studies, a contact network is usually represented in a multilayer setting where the agents interact through different layers, each modeled by a separate graph (Sahneh & Scoglio, 2013; Sahneh, Scoglio, & Chowdhury, 2013a; Sahneh et al., 2013b; Shakeri et al., 2015; Xia et al., 2019). For example, the spontaneous behavioral patterns of individuals in response to the progress of an epidemic, which have a significant impact on how the infection spreads (Shakeri et al., 2015), form through an information network layer that is interconnected with, but different from, the physical contact network layer (Sahneh et al., 2014; Sahneh & Scoglio, 2012). This interconnection between different network layers is interwoven. For example, the spectral centrality of the nodes and edges in the physical contact network determines the optimal information dissemination network (Sahneh & Scoglio, 2012).

In this study, we present a deterministic approximation of stochastic viral marketing (i.e., an epidemic) dynamics using mean field theory. The deterministic models have offered remarkable analytical results for nonlinear characterization of equilibria, stability properties, and threshold conditions in epidemic models (Hethcote, 2000). In Fall et al. (2007), the Lyapunov techniques (Khalil, 2014) and Metzler matrix theory (Bullo, 2019) are utilized to establish existence, uniqueness, and stability of the equilibrium points below and above the epidemic threshold over networks. The epidemic goes extinct by converging to the zero-state epidemic-free equilibrium below the threshold while propagating by converging to a positive endemic equilibrium above the threshold. These results are extended to epidemic dynamics over directed graphs by utilizing the positive system theory (Khanafer, Başar, & Gharesifard, 2016). A further extension of primary results is found in (Ogura & Preciado, 2018) where, in search of tighter epidemic thresholds, a deterministic network with second-order mean field approximation is analyzed. A review of mathematical analysis of deterministic networked epidemic models is found in Mei, Mohagheghi, Zampieri, and Bullo (2017).

Early epidemic models were based on the assumption that individuals in the population have the same chances of interacting with each other (Hethcote, 2000). This strategy is suitable for a well-mixed homogenous population and overlooks the internal structure of the network over which the propagation occurs (Sahneh & Scoglio, 2012). To model the local dynamics at each node, and to discover how interaction among population members can influence spreading dynamics, individual-based epidemic models were proposed where a graph represents the contact network. In a modern mathematical language, the influence of the network characteristics on the information spread can be demonstrated through an N-intertwined Markov chain model (Van Mieghem et al., 2009a). The spectral radius of the network is found as one determining factor in the epidemiological spreading so that for a small spectral radius, an initial infection ceases to spread, while even tiny infections diffuse for spectral radius larger than a threshold.

Epidemic dynamics has proven effective in studying various phenomena related to the spread process in networks. Studies in epidemic dynamics range from the spread of infectious diseases to the spread of information, rumor, cultural norms, computer viruses, social behavior, and disasters (Hu & Sheng, 2015; Kiss et al., 2017; Urena, Kou, Dong, Chiclana, & Herrera-Viedma, 2019; Van Mieghem et al., 2009a; Yang, Li, & Giua, 2020; Yu et al., 2015). Although the underlying mechanisms of each phenomenon are different, their mathematical description often leads to similar constitutive equations that can be conceptually modeled as a contagion process based on classic epidemic models such as the susceptible-infected-susceptible (SIS) and susceptible-infected-recovered (SIR) models (Antulov-Fantulin, Lančić, Štefančić, & Šikić, 2013; Kiss et al., 2017). While network-related frameworks are extensively utilized to study the viral marketing strategies and influence maximization problems, to the best of our knowledge, dynamic epidemic models are not considered in the context of incentive rate determination. In this study, we examine the IRD problem in a network of consumers to establish a new dynamic model that is based on epidemic spreading dynamics. Our goal is first to discover how the connection and interaction between individuals who can be incentivized to behave as sales agents

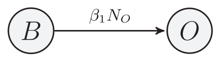

Fig. 1. BO model.

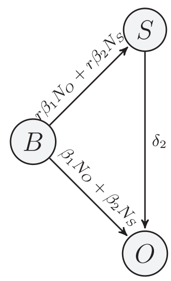

Fig. 2. BOSO model.

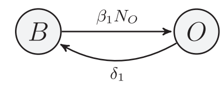

Fig. 3. BOB model.

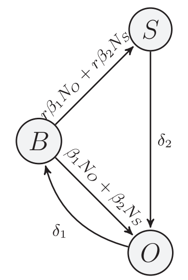

Fig. 4. BSOB model.

can affect the marketing of a product or service. Then, we will investigate incentive control policies that can maximize the profit by affecting the decision process of individuals.

3. Model development

The contact topology in this paper is considered as an undirected generic graph $\mathcal{G}(\mathcal{V}, \mathcal{E})$ of individuals where $\mathcal{V}$ denotes the vertex set and $\mathcal{E}$ denotes the edge set. Each node $i \in \mathcal{V}$ is allowed to be in one of the three states "B: buyer", "O: owner", and "S: seller". We denote the probability of $i \in \mathcal{V}$ being in B as $b_i \in [0, 1]$, in O as $p_i \in [0, 1]$, and in S as $q_i \in [0, 1]$. In the remainder of this section, first, we describe some initial possible models for the spread of information and sales over networks. Then, we introduce our Buyer-Seller-Owner-Buyer (BSOB) model.

3.1. Irreversible process

One straightforward approach to model a good's sale under network externalities is to assume an irreversible process in which each individual is either in state B or O and a consumer stays in state O after transitioning to it from state B. This dynamic is similar in nature to a susceptible-infected (SI) model in epidemiology and may perform reasonably for goods that are purchased once and have negligible probability of being repurchased by a consumer. The stochastic compartmental transition of a node with N_O neighbors in owner state is depicted in Fig. 1. We call this model as Buyer-Owner (BO) model. In BO model, the rate by which a potential buyer becomes owner is β_1 times the number of an individual's neighbors who are in owner state (i.e. N_O) where β_1 represents the network externality effect originated from owners. Since BO models an irreversible process, it can be used to estimate the survival duration of a good's sales under network externalities.

To accelerate the diffusion process, the irreversible BO model may be extended to include the third compartment of seller, called Buyer-Owner-Seller-Owner (BOSO). The individuals in seller state receive an incentive to promote the good and encourage their neighbors, who are in state B, to purchase the good. Compartmental transition of BOSO is shown in Fig. 2. Here, the rate of a potential buyer becoming an owner is β_1 times the number of its owner neighbors, N_O, plus β_2 times the number of its seller neighbors, N_S. Here, β_1 and β_2 represent the externality effects originated from owners and sellers in a network. The effect of incentive is modeled through a factor r that augments the transition rate from state B to S. The factor δ_2 is the rate of transitioning from state S to O and corresponds with the suspension of the good's promotion by an individual. We assume that sellers have higher impact on their neighbors compared to owners (i.e. $\beta_2 > \beta_1$). Similar to the BO model, BOSO can be applied to a sales survival estimation, in which some individuals are willing to promote the good if incentivized.

3.2. Reversible process

To model a scenario in which a good can be consumed more than once, BO and BOSO models need to be modified so that an individual can transition back to a potential buyer state. The BO model can be extended to a buyer-owner-buyer (BOB) model that encompasses a transition from the state O to B with a rate of δ_1. BOB model closely follows the well-known N-intertwined Susceptible-Infected-Susceptible (SIS) model for epidemic spread (Wang, Chakrabarti, Wang, & Faloutsos, 2003). The transition diagram of BOB model is shown in Fig. 3. In this model, a potential buyer becomes owner by an edge-based transition equal to β_1 times the number of its owner neighbors, and an owner returns to the buyer state with the nodal transition rate δ_1. Using $b_i + p_i = 1$, the N-intertwined equation is written as (see Appendix B):

$$\dot{p}_i = (1 - p_i)\beta_1 \sum_j a_{ij} p_j - \delta_1 p_i \tag{1}$$

where $A = \left[a_{ij}\right] \in \mathbb{R}^{N \times N}$ is the network adjacency matrix. Based on model (1), the probability being owner, $p_i(t)$, will die out exponentially if the spreading strength $\tau \triangleq \frac{\beta_1}{\delta_1}$ satisfies $\tau \triangleq \frac{\beta_1}{\delta_1} \leqslant \frac{1}{\rho(A)}$, where $\rho(A)$ is the spectral radius of the adjacency matrix. Therefore, for the BOB model, the trading continues in steady state if and only if (Wang et al., 2003)

$$\tau = \frac{\beta_1}{\delta_1} > \tau_c = \frac{1}{\rho(A)} \tag{2}$$

If (2) is satisfied, the steady state values of the owner probabilities, denoted by $\bar{p}_i$ for the i-th individual, are the non-trivial solution of the following set of equations:

$$\frac{\beta_1}{\delta_1} \sum_j a_{ij} \bar{p}_j = \frac{\bar{p}_i}{1 - \bar{p}_i} \tag{3}$$

3.3. Buyer-seller-owner-buyer model

In this study, we extend the BOB to an N-intertwined BSOB model by augmenting a seller compartment to the transition diagram (Fig. 4). Similar to the BOSO model, transitioning to the seller state depends on an incentive rate r. In BSOB, a potential buyer becomes owner by β_1 times the number of its owner neighbors plus β_2 times the number of its seller neighbors. An owner recovers back to the buyer state by the nodal transition of rate δ_1. Potential buyers who are aware of the incentive r, may be encouraged to become seller, and in turn influence their neighbors to buy the good. In this regard, a potential buyer will go to the seller state with the rate it goes to the owner sate times r. The sellers then go to the owner state by the nodal transition of rate δ_2. Since the seller individuals affect their potential buyer neighbors actively, it should be that $\beta_2 > \beta_1$, which indicates the sellers are more influential in persuading their neighbors than the owner individuals are. Naturally, an owner cannot become seller without buying the good. Thus, there is no direct transition from the owner state to the seller state. Furthermore, we assume that transition from a seller individual to a potential buyer state is much slower than other transitions. Hence, in our modeling setup, a seller never goes back directly to the buyer state.

For each node $i \in \{1, \dots, N\}$, let us define a random variable $X_i : \{B, O, S\}$, and denote X_i^t the value of X_i at time t. The epidemic spread dynamics of BSOB is modeled as the following continuous-time Markov process:

$$\begin{aligned}
&\Pr\left(X_i^{t+\Delta t} = O | X_i^t = B, \boldsymbol{X}^t\right) = \beta_1 \Delta t Y_i^t + \beta_2 \Delta t Z_i^t + o(\Delta t)\\
&\Pr\left(X_i^{t+\Delta t} = S | X_i^t = B, \boldsymbol{X}^t\right) = r\beta_1 \Delta t Y_i^t + r\beta_2 \Delta t Z_i^t + o(\Delta t)\\
&\Pr\left(X_i^{t+\Delta t} = B | X_i^t = O, \boldsymbol{X}^t\right) = \delta_1 \Delta t + o(\Delta t)\\
&\Pr\left(X_i^{t+\Delta t} = O | X_i^t = S, \boldsymbol{X}^t\right) = \delta_2 \Delta t + o(\Delta t)
\end{aligned} \tag{4}$$

where $i \in \{1, \dots, N\}$, $Y_i^t \triangleq \sum_{j\in\mathcal{N}_i} a_{ij} 1_{\{X_j^t = O\}}$, and $Z_i^t \triangleq \sum_{j\in\mathcal{N}_i} a_{ij} 1_{\{X_j^t = S\}}$, with $1_{\{\mathcal{X}\}}$ being the indicator function. In (4), Pr(.) denotes probability, $\boldsymbol{X}^t \triangleq \{X_i^t, i = 1, \dots, N\}$ is the joint state of the network, and Δt is a time step. Using a proper mean field approximation, it is possible to express the transition probabilities in terms of the corresponding expected values. Specifically, the terms $1_{\{X_j^t = O\}}$ and $1_{\{X_j^t = S\}}$ are, respectively, replaced with $\mathrm{E}[1_{\{X_j^t = O\}}]$ and $\mathrm{E}[1_{\{X_j^t = S\}}]$, where E[.] denotes the expected value. Then, using the fact that p_i, q_i, and b_i are not independent, since $b_i + p_i + q_i = 1$, we obtain the N-intertwined equation as:

$$\begin{aligned}
\dot{p}_i &= (1 - p_i - q_i)\left(\beta_1 \sum_j a_{ij} p_j + \beta_2 \sum_j a_{ij} q_j\right) - \delta_1 p_i + \delta_2 q_i\\
\dot{q}_i &= r(1 - p_i - q_i)\left(\beta_1 \sum_j a_{ij} p_j + \beta_2 \sum_j a_{ij} q_j\right) - \delta_2 q_i
\end{aligned} \tag{5}$$

Eq. (5) is written in vector form as

$$\begin{aligned}
\dot{p} &= (I - P - Q)(\beta_1 A p + \beta_2 A q) - \delta_1 p + \delta_2 q\\
\dot{q} &= r(I - P - Q)(\beta_1 A p + \beta_2 A q) - \delta_2 q
\end{aligned} \tag{6}$$

where $p_{N\times 1} = [p_1, \dots, p_N]^T$, $q_{N\times 1} = [q_1, \dots, q_N]^T$, $P_{N\times N} = \mathrm{diag}(p)$, $Q_{N\times N} = \mathrm{diag}(q)$, and I is the identity matrix with appropriate dimension.

Remark 1. It can be easily verified that, the set $[0,\ 1]^{2N}$ is a compact positively invariant set for system (6). In fact, it can be concluded from (5) that starting from an initial condition p_i, $q_i \in [0,\ 1]$, neither p_i nor q_i can become less than zero. This is because $\dot{p}_i \geq 0$ when $p_i = 0$ and $\dot{q}_i \geq 0$ when $q_i = 0$. Moreover, taking $s_i = p_i + q_i$, we have from (5) $\dot{s}_i = (r + 1)(1 - s_i)\big(\beta_1 \sum_j a_{ij} p_j + \beta_2 \sum_j a_{ij} q_j\big) - \delta_1 p_i$. This indicates $\dot{s}_i < 0$ when $s_i = 1$, for p_i, $q_i > 0$. Therefore, s_i can never exceed 1 when starting from an initial condition $s_i < 1$.

Remark 2. From (6), by $b_i + p_i + q_i = 1$, we note that

$$\begin{aligned}
\dot{p} &= B(\beta_1 A p + \beta_2 A q) - \delta_1 p + \delta_2 q\\
\dot{b} &= -(r + 1)B(\beta_1 A p + \beta_2 A q) + \delta_1 p
\end{aligned}$$

with $B = \mathrm{diag}(b)$, $b_{N\times 1} = [b_1, \dots, b_N]^T$. For nonnegative states and $r > 0$, we observe that $-\dot{b} \geq \beta_1 B A p - \delta_1 p$. The right hand side of this inequality is nothing but the BOB dynamics demonstrated in (1). In fact, denoting by $\hat{(.)}$ the states in the BOB model, it follows that $-\dot{\hat{b}} = \dot{\hat{p}} = \beta_1 \hat{B} A \hat{p} - \delta_1 \hat{p}$, so that $-\dot{b}(t) \geq -\dot{\hat{b}}(t)$. Therefore, when the two systems start from the same initial conditions, the decrease of Buyers in the BOB is slower than is in BSOB. This shows that, the probability of remaining in Buyer state is smaller in BSOB than is in BOB. In other words, compared to the BOB model, sellers help to generate more sales.

4. Equilibrium states: homogeneous incentive values

4.1. Trade-free equilibrium

In this subsection, we investigate the stability of the trivial equilibrium point $\left[p^T q^T\right]^T = 0$ of (6). In such conditions, the individuals will steadily remain in Buyer state after a transient time and there will be no trading (i.e. no transition from B to S or O) in steady state. The main outcomes of this subsection are as follows. First, by studying the spectrum of the model, we derive the stability conditions for the zero state in Theorem 1. We then determine in Eq. (11) the minimum incentive required to destabilize the trade-free equilibrium and establish active trading in steady state. The minimum incentive is important as it determines a threshold, above which individuals continue transitioning from state B to states S or O and generate sale while below this threshold, no sales will be generated after a certain amount of time elapsed. We also determine an explicit expression for the reproduction number in Eq. (12). Henceforth, $\lambda_1(.)$ will denote the largest eigenvalue of corresponding matrix argument.

Proposition 1. *Consider the N-intertwined BOSB model (5). Then if*

$$\lambda_1(\mathcal{A}) \leq -\epsilon, \quad \epsilon > 0 \tag{7}$$

where

$$\mathcal{A} = \begin{bmatrix} \beta_1 A - \delta_1 I & \beta_2 A + \delta_2 I \\ r\beta_1 A & r\beta_2 A - \delta_2 I \end{bmatrix} \tag{8}$$

an initial condition $[p^T(0)\, q^T(0)]^T \in [0,\ 1]^{2N}$ will converge to zero exponentially fast.

Proof of Proposition 1. See A.1 □

Proposition 2. *The spectrum of $\mathcal{A}$ is given in terms of spectrum of A as*

$$\begin{aligned}
2\lambda(\mathcal{A}) = &-[\delta_1 + \delta_2 - (\beta_1 + r\beta_2)\lambda(A)]\\
&\pm\sqrt{[(\delta_1 - \delta_2) - (\beta_1 - r\beta_2)\lambda(A)]^2 + 4r\beta_1[\delta_2 + \beta_2\lambda(A)]\lambda(A)}
\end{aligned} \tag{9}$$

where the notation λ(.) denotes the eigenvalue of the corresponding matrix, so that $\lambda = \lambda(\mathcal{A})$. Therefore, for each eigenvalue of A we get two eigenvalues for $\mathcal{A}$, i.e., the total number of 2N eigenvalues for $\mathcal{A}$. Moreover, since the eigenvalues of the adjacency matrix A are all real, since it is symmetric for undirected graphs, Eq. (9) indicates that the eigenvalues of $\mathcal{A}$ are real as well.

Proof of Proposition 2. See A.2 □

Theorem 1. *The trivial equilibrium of the N-intertwined BOSB model (5) is globally exponentially stable if and only if*

$$(r + 1)\frac{\beta_1}{\delta_1} + r\frac{\beta_2}{\delta_2} < \frac{1}{\lambda_1(A)} \tag{10}$$

Proof of Theorem 1. See A.3 □

To have an active trading (i.e. sales) in steady state, the trivial equilibrium point should be unstable. By the assistance of (10), we conclude that for trading to continue in steady state, the incentive should be lower-bounded as $r > r_c$ where

$$r_c = \left(\frac{\beta_1}{\delta_1} + \frac{\beta_2}{\delta_2}\right)^{-1}\left(\frac{1}{\lambda_1(A)} - \frac{\beta_1}{\delta_1}\right) \tag{11}$$

The threshold r_c is the minimum incentive required to make steady profit in a viral marketing campaign. Below this threshold, sales will eventually diminish while above this threshold, sales will continuously exist as individuals are incentivized enough to promote the good and collect profit upon sales. Eq. (11) shows that the incentive threshold r_c is conversely related to $\lambda_1(A)$, β_1/δ_1, and β_2/δ_2. Therefore, when the spectral radius $\lambda_1(A)$ or the externality effects β_1 and β_2 are small, larger incentives are required for active trading. Moreover, smaller recovery rates δ_1 and δ_2 translate to a smaller incentive threshold r_c.

Following the epidemiology literature, we can define the reproduction number $\mathcal{R}_0$, as the expected number of new transitions to O or S states caused by a typical individual in owner or seller state within a population of potential buyers only. Many conventional results have demonstrated the global stability of the trade-free equilibrium when $\mathcal{R}_0 < 1$. By this convention, we conclude from the stability condition in (10) that the basic reproduction for the proposed BSOB is given as

$$\mathcal{R}_0 = \left[(r+1)\frac{\beta_1}{\delta_1} + r\frac{\beta_2}{\delta_2}\right]\lambda_1(A) \tag{12}$$

It is observed that, $\mathcal{R}_0$ is an increasing linear function of the incentive r with slope $(\beta_1/\delta_1 + \beta_2/\delta_2)\lambda_1(A)$. By setting $r = 0$, we reach the reproduction number $\beta_1/\delta_1\lambda_1(A)$ in the BOB model. Therefore, in comparison to the BOB model, with the reproduction number $\beta_1/\delta_1\lambda_1(A)$, we observe from (12) that the BSOB model holds a larger reproduction number. This expedites the spread process in the BSOB. Another consequence is that, the BSOB trade-free equilibrium is stable in a narrower band of the parameters. That is to say, compared to the BOB, the trade-free equilibrium in the BSOB becomes unstable under weaker contact characteristics, i.e. it is unstable in smaller $\lambda_1(A)$ and/or smaller β_1/δ_1. From a marketing perspective and compared to a no-incentive scenario, this means a viral marketing campaign that incentivizes individuals to act as sales agents can facilitate sales generation in networks with lower number of contacts between individuals.

4.2. Endemic equilibrium

In this subsection, we investigate the existence and stability conditions of endemic equilibrium state where transitions between the states B, O and S occur continuously. This means the network externality effect is influential enough to keep the individuals motivated for changing states. The main results of this subsection are found in Lemmas 1,3 and Theorem 2, where we show that for values of reproduction number greater than one, i.e. $\mathcal{R}_0 > 1$, there is a unique endemic equilibrium that is strongly positive and globally asymptotically stable. We also suggest a convergent sequence in (19) to calculate the endemic equilibrium.

The nontrivial equilibrium point $\left[\bar{p}^T\ \bar{q}^T\right]^T$ is obtained by setting in (6) $\dot{p} = \dot{q} = 0$:

$$\begin{aligned}&\left(I - \bar{P} - \bar{Q}\right)(\beta_1 A\bar{p} + \beta_2 A\bar{q}) - \delta_1\bar{p} + \delta_2\bar{q} = 0\\ &r\left(I - \bar{P} - \bar{Q}\right)(\beta_1 A\bar{p} + \beta_2 A\bar{q}) - \delta_2\bar{q} = 0\end{aligned} \tag{13}$$

where $\bar{P} = \mathrm{diag}(\bar{p})$ and $\bar{Q} = \mathrm{diag}(\bar{q})$. Multiplying the first of (13) by r and subtracting the result from the second equality, we have

$$\bar{q} = \frac{r\delta_1}{(r+1)\delta_2}\bar{p} \tag{14}$$

Inserting (14) into the second of (13), we obtain the following nonlinear equation for $\bar{p}$

$$\left[\frac{\beta_1}{\delta_1}(r+1) + r\frac{\beta_2}{\delta_2}\right]^{-1}\bar{p} = \left[I - \frac{r\delta_1 + (r+1)\delta_2}{(r+1)\delta_2}\bar{P}\right]A\bar{p} \tag{15}$$

Lemma 1. *Any endemic equilibrium is strongly positive, $[\bar{p}^T\ \bar{q}^T]^T \gg \mathbf{0}$, where $\mathbf{0}$ is the zero vector. Therefore, in an equilibrium state, either all elements of the vector $[\bar{p}^T\ \bar{q}^T]^T$ are zero, or no element has a zero value.*

Proof of Lemma 1. See A.4 □

Lemma 1 indicates that in an equilibrium state, either all individuals have nonzero probabilities of purchasing the good, or no one purchases the good at all. Since $\bar{p} \gg 0$, and so $A\bar{p} \gg 0$ for a connected graph, Eqs. (14) and (15) indicate that every endemic equilibrium satisfies

$$\begin{aligned}\bar{p}_i &< \bar{p}_{max}(r) \triangleq \frac{(r+1)\delta_2}{r\delta_1 + (r+1)\delta_2},\\ \bar{q}_i &< \bar{q}_{max}(r) \triangleq \frac{r\delta_1}{r\delta_1 + (r+1)\delta_2}\end{aligned} \tag{16}$$

Therefore, any solution of (14) and (15) is smaller than 1, $\bar{p}, \bar{q} \ll \mathbf{1}$, where $\mathbf{1}$ is all ones vector. Moreover, in an irreversible process, where $\delta_1 = 0$, we have $\bar{q}_{max}(r) = 0$, indicating a steady state in which the probability of being a seller is zero. In such a steady state, since transitioning to the seller compartment is possible only from the potential buyer compartment, we can conclude that the probability of being a potential buyer is zero as well. Thus, in an irreversible process shown in Fig. 2, starting from a nonzero initial condition, all individuals will eventually wind up in the owner state. As r in (16) goes to infinity, we have

$$\lim_{r\to\infty}\bar{p}_i < \bar{p}_\infty \triangleq \tfrac{\delta_2}{\delta_1+\delta_2},\quad \lim_{r\to\infty}\bar{q}_i < \bar{q}_\infty \triangleq \tfrac{\delta_1}{\delta_1+\delta_2} \tag{17}$$

that shows for extremely large incentive values, the only determining factors of the steady state bound are δ_1 and δ_2, which implies a diminishing role of the underlying network structure as the incentive rate increases.

Lemma 2. *The existence of any endemic equilibrium is subject to $\mathcal{R}_0 > 1$.*

Proof of Lemma 2. See A.5 □

Using (12), the endemic equilibrium condition (15) may be rearranged as

$$\bar{p} = \left[\mathrm{diag}\left(\mathbf{1} + \frac{a\mathcal{R}_0}{\lambda_1(A)}A\bar{p}\right)\right]^{-1}\frac{\mathcal{R}_0}{\lambda_1(A)}A\bar{p} \tag{18}$$

where $a = \frac{r\delta_1 + (1+r)\delta_2}{(r+1)\delta_2} > 1$. To reach (18), we have considered that $\bar{P}A\bar{p} = \mathrm{diag}(A\bar{p})\bar{p}$.

Lemma 3. *There is a unique endemic equilibrium when $\mathcal{R}_0 > 1$.*

Proof of Lemma 3. See A.6. □

Remark 3. The proof of Lemma 3 in A.6 provides us with a convergent sequence to calculate the endemic equilibrium. Indeed, under the initial condition $y(0)$ a scalar multiple of u_1, with u_1 being the eigenvector corresponding to λ_1 and $a\max_i y_i(0) \le 1 - 1/\mathcal{R}_0$, the sequence $\{y(k)\}_{k\in\mathbb{N}} \subset \mathbb{R}^N$,

$$y(k+1) = F\left(\frac{\mathcal{R}_0}{\lambda_1}Ay(k)\right) \tag{19}$$

where $[F(y)]_i = \frac{y_i}{1+ay_i}$, $a = \frac{r\delta_1+(1+r)\delta_2}{(r+1)\delta_2}$, converges to $\bar{p}$:

$$\lim_{k\to\infty} y(k) = \bar{p}$$

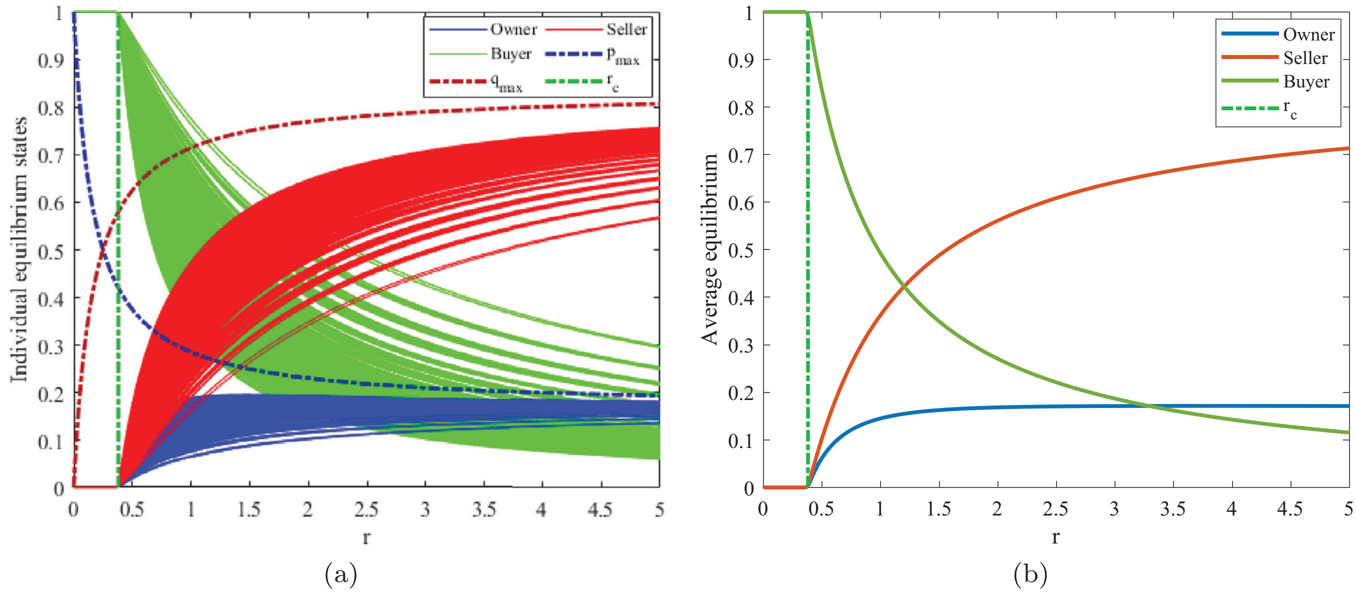

Fig. 5. (a) Individual, and (b) average, equilibrium states.

We can additionally relax the initial condition $y(0)$ being a scalar multiple of u_1 since we have already proved the endemic equilibrium is unique. Hence, by starting from any initial condition $\mathbf{0} \neq y(0) \in [0,\,1]^N$, it is expected the series (19) converges to $\bar{p}$.

Theorem 2. *Suppose that $\mathcal{R}_0 > 1$. Then the endemic equilibrium is globally asymptotically stable.*

Proof of Theorem 2. See A.7. □

Fig. 5 shows the equilibrium of the BOSB for different values of incentive factor r in an Erdos–Renyi network with 1000 nodes and the connection probability 0.0138 ($\lambda_1(A) = 14.938$). The numerical values are $\delta_1 = 1, \delta_2 = .2, \beta_1 = 0.0175, \beta_2 = 0.0225$. As it can be observed, for incentive factors below r_c, only the trade-free equilibrium is possible. After this critical incentive, the probabilities of settling into owner and seller states increase monotonically and for larger incentives r converge to values associated with (17), while the probability of being a potential buyer decreases monotonically for $r > r_c$. Fig. 6 presents the time response of BSOB for $r = 2 > r_c$ where GEMF simulator (Sahneh, Vajdi, Shakeri, Fan, & Scoglio, 2017) is used to track the behavior of the stochastic model (4) over time. As it can be observed in the example of Fig. 6, mean field closely follows the Markov process. It is noteworthy that in some instances, such as the ones investigated by Van Mieghem, Omic, and Kooij (2009b), the mean filed approximation error may grow.

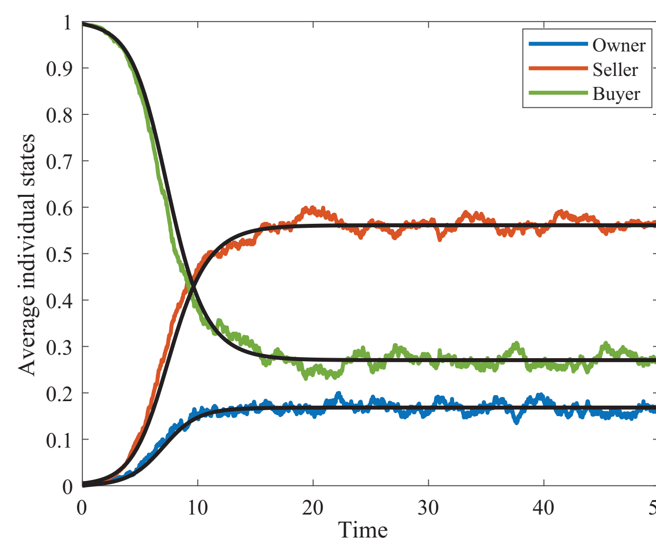

Fig. 6. The number of individuals in Owner, Seller, and Buyer states at each time for a given initial condition for the BSOB model (4) obtained by GEMF simulator in an Erdos–Renyi graph with 1000 nodes (the black lines represent the mean field approximation (5)).

5. Maximizing profit: homogeneous incentive values

5.1. *Profit function: evidence of existence of an optimal incentive* r*

Every time an individual transitions to the state O or S, a certain amount of profit is generated. The sales profit generated during a time period T can be defined as

$$\Pi(r) = \Pi_0 n_{B\to O} + (\Pi_0 - f(r)) n_{B\to S} \tag{20}$$

where $n_{B\to O}$ and $n_{B\to S}$ represent the number of transitions from potential buyer to owner and seller states during the time period T, respectively, and Π_0 is the profit due to a single transition from Buyer to Owner. In (20), the function $f(r)$ is the incentive given to potential buyers to encourage their transition to the seller state, and is a non-decreasing function of the incentive factor r. In the simplest scenario, we may suppose the incentive value is a linear function of the incentive factor r through a constant coefficient κ, i.e. $f(r) = \kappa r$. In other words, it is supposed that the probability of a potential buyer becoming a seller grows linearly with the amount of the incentive given through the coefficient κ. For the mean field model (5), the expected profit is computed as

$$\mathrm{E}[\Pi(r)] = \Pi_0 \mathrm{E}[n_{B\to O}] + (\Pi_0 - f(r)) \mathrm{E}[n_{B\to S}] \tag{21}$$

In general, the expected transitions during the time period T are obtained according to the transition digraph 4 as

$$\begin{aligned}\mathrm{E}[n_{B\to O}] &= \frac{1}{r}\mathrm{E}[n_{B\to S}] \\ &= \int_0^T \sum_i (1 - p_i - q_i)\left(\beta_1 \sum_j a_{ij} p_j + \beta_2 \sum_j a_{ij} q_j\right) dt\end{aligned} \tag{22}$$

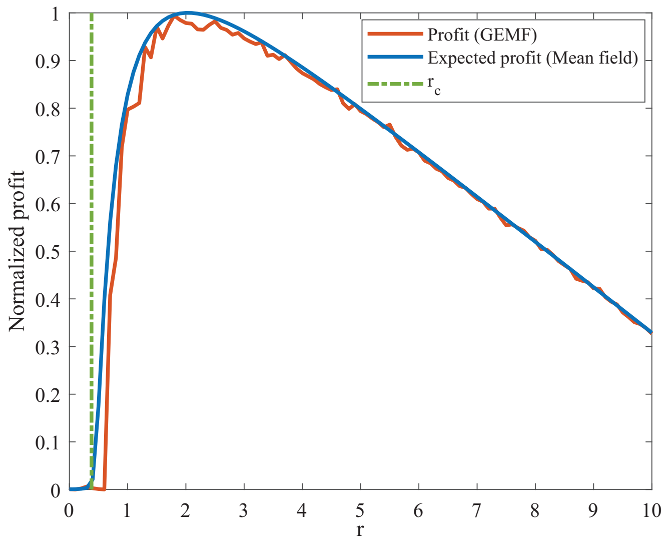

Fig. 7. The profit as a function of the incentive factor in an Erdos–Renyi graph with 1000 nodes calculated for the time period $\boldsymbol{T = 100}$.

Fig. 7 shows the normalized profit as a function of the incentive factor r in an Erdos–Renyi graph with 1000 nodes. Here, the incentive was computed for $\kappa = 2$ and the time period $T = 100$, and was normalized by making the maximum profit equal to 1. As illustrated by Fig. 7, before the incentive threshold r_c, the profit is almost zero (some minor profit is expected in transient due to the initial conditions). The profit starts to grow after the threshold, until it reaches its maximum value at an incentive value $r^*(T)$ and then starts to decrease with increasing incentive.

Fig. 8 depicts various transitions and the number of their occurrences for different values of incentive r in an artificial example when $T = 100$. The number of transitions below the threshold r_c is practically zero (there are only few transitions during the transient period). Above the threshold r_c, all transitions, but the transition from a potential buyer to owner, are non-decreasing functions of the incentive. However, the transition from B to O reaches a maximum value at an incentive amount less than r^*. After the threshold r_c, the transition from B to O grows due to increased number of sellers who are willing to promote the good and generate sales. However, after a certain incentive value, for which the number of transitions from B to O reaches its maximum, the incentive amount given is large enough to encourage the potential buyers to dominantly become sellers, rather than owners. Thus, the number of transitions from a potential buyer to an owner decreases. Considering these observations, one can conclude that the profit increases after r_c due to an escalated level of transitions from B to O and S. Furthermore, the profit starts to deteriorate after r^* due to the excessive amount of incentive given (over-incentivization) and as a result, reduced number of transitions from B to O.

5.2. Maximizing the steady state profit: nonlinear programming

To find the maximum profit over a time period T (i.e. $r^*(T)$) We can optimize the profit function (20) subject to the stochastic model (4), or by mean field approximation, optimize (21) subject to (5). These optimization models, result in stochastic and deterministic optimal control problems, and the corresponding dynamic programmings. An alternative approach is to maximize the steady state profit. For this purpose, and considering $\mathrm{E}[n_{B\to S}] = r\mathrm{E}[n_{B\to O}]$ in (22), we observe that the expected profit in (21) may be rewritten as $\mathrm{E}[\Pi(r)] = [\Pi_0(r+1) - rf(r)]\mathrm{E}[n_{B\to O}]$. By (22), we know that the expected number of transitions from state B to O at each time step Δt is $(\mathbf{1} - p - q)^T(\beta_1 Ap + \beta_2 Aq)\Delta t$. Thus, the expected profit at each time step becomes $[\Pi_0(r+1) - rf(r)](\mathbf{1} - p - q)^T(\beta_1 Ap + \beta_2 Aq)\Delta t$. To maximize the profit in steady state, the dynamics constraint (6) needs to be replaced with the static equilibrium condition (13), or equivalently, by (14) and (15). We may utilize (13) to express the expected profit at each time step under endemic equilibrium condition as $\delta_1(\Pi_0 - r/(r+1)f(r))\mathbf{1}^T\bar{p}\Delta t$, where $\bar{p}$ is subjected to satisfy the nonlinear constraint (15). By this argument, we consider the following nonlinear programming for maximizing the profit in the steady state:

$$\max_{r,\bar{p}} \quad \left(\Pi_0 - \frac{r}{r+1}f(r)\right)\mathbf{1}^T\bar{p}$$
$$\text{s.t.} \begin{cases} \left[\dfrac{\beta_1}{\delta_1}(r+1) + r\dfrac{\beta_2}{\delta_2}\right]^{-1}\bar{p} = \left[I - \dfrac{r\delta_1 + (r+1)\delta_2}{(r+1)\delta_2}\bar{P}\right]A\bar{p} \\ r \geq 0 \end{cases} \tag{23}$$

By Lemma 3, we know that, for each $r \geq r_c$, there exists a unique $\bar{p}$ that satisfies the equality constraint in (23). Hence, the feasible set of the optimization problem is nonempty. In addition, if we suppose $f(r)$ is such that $r/(r+1)f(r)$ is convex for $r > 0$, the cost function $(\Pi_0 - r/(r+1)f(r))\mathbf{1}^T\bar{p}$ will be concave. This shows that (23) holds a unique optimal solution, which may be obtained using the Interior-Point (IP) or Sequential Quadratic Programming (SQP) approaches (Nocedal & Wright, 2006). Note that by (23), we neglect the transient profit. This is meaningful if the transient trading is not significant compared to the steady state trading. This is also the case when the profit is to be maximized for a sufficiently large time period T.

Denoting the solution of (23) as $(r_s^*, \bar{p}^*)$, Fig. 9 shows the optimal incentive values $r^*(T)$ and their corresponding endemic equilibrium for different time periods T. We observe that, by increasing the time period T, during which the profit is computed, the optimal incentive uniformly approaches r_s^* from above. The manner by which different optimal incentives converge in Fig. 9 guide us to a control strategy, in which we start by a maximum possible incentive for optimal profit in transient, gradually reduce the incentive as time goes on, and finally switch to the incentive r_s^* for optimal profit in the steady state (i.e. the solution of (23)). As Fig. 9 shows, for optimum incentive value in the steady state, probability of being in state S is higher than the probability of being in each state B or O.

6. Equilibrium states: heterogeneous incentive values

Depending on their position in a network, individuals wield a different degree of influence in information diffusion. Thus, it may seem natural to assign different incentive values to individuals based on the amount of influence they can exert, which is usually quantified in the form of centrality measures. The most basic and trivial centrality measure may be the number of neighbors an individual has. However, since the importance of an individual can be measured through various definitions, there are many different definitions of centrality (Liao, Mariani, Medo, Zhang, & Zhou, 2017; Nasirian, Pajouh, & Balasundaram, 2020). Therefore, to identify essential qualities and quantities for determining an important individual in a viral marketing campaign, we consider the case of heterogeneous incentive values in the BSOB model and investigate its dynamics properties. Then, we will examine the problem of profit maximization with heterogeneous incentive values. One of the main results of this section is expressed in Theorem 3 where we derive the exponential stability conditions of the trade-free equilibrium in terms of the reproduction number (27). Then we express the existence and stability conditions of a unique endemic equilibrium in Lemmas 5 and 6. We also demonstrate by

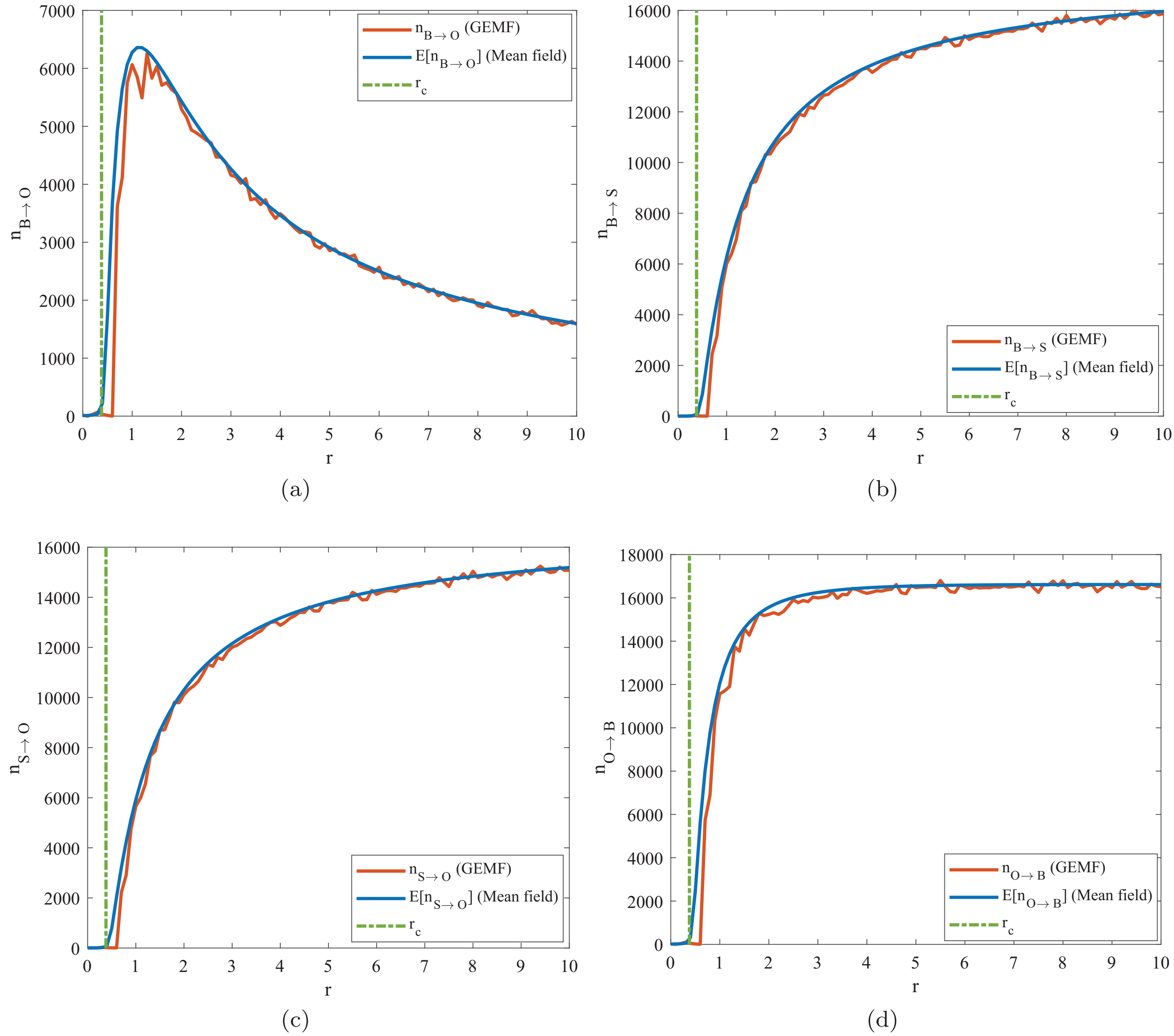

Fig. 8. The number of transitions from (a) potential buyer to owner, (b) potential buyer to seller, (c) seller to owner, and (d) owner to potential buyer.

Lemma 7 how large the value of standard deviation in incentive distribution should be to have an active steady state trading when the average incentive is smaller than the threshold r_c in (11).

When different agents can receive different incentives, we consider the following mean field dynamics:

$$\dot{p}_i = (1 - p_i - q_i)\left(\beta_1 \sum_j a_{ij} p_j + \beta_2 \sum_j a_{ij} q_j\right) - \delta_1 p_i + \delta_2 q_i$$
$$\dot{q}_i = r_i (1 - p_i - q_i)\left(\beta_1 \sum_j a_{ij} p_j + \beta_2 \sum_j a_{ij} q_j\right) - \delta_2 q_i \qquad (24)$$

where r_i denotes the incentive factor corresponding to the ith individual. In vector form we have

$$\dot{p} = (I - P - Q)(\beta_1 Ap + \beta_2 Aq) - \delta_1 p + \delta_2 q$$
$$\dot{q} = R(I - P - Q)(\beta_1 Ap + \beta_2 Aq) - \delta_2 q \qquad (25)$$

where $R = \text{diag}([r_i])$, or $R = \text{diag}(\boldsymbol{r})$ where $\boldsymbol{r}$ denotes the incentive factor vector with components r_i. Similar to Remark 1, it can be verified that the set $[0, 1]^{2N}$ is a compact positively invariant set for (25). To establish the main results in this section, we introduce the reproduction matrix $\mathcal{R} = \text{diag}([\mathcal{R}_i])$ as a diagonal matrix with the following positive pivot entries:

$$\mathcal{R}_i = (r_i + 1)\frac{\beta_1}{\delta_1} + r_i \frac{\beta_2}{\delta_2} \qquad (26)$$

The reproduction number in the heterogeneous incentive is the largest eigenvalue of the matrix $\mathcal{R}A$:

$$\mathcal{R}_0 = \lambda_1(\mathcal{R}A) \qquad (27)$$

Note that since A is Metzler irreducible[2] and $\mathcal{R}$ is diagonal with positive pivot entries, $\mathcal{R}A$ is Metzler irreducible. Hence, the largest eigenvalue of $\mathcal{R}A$ and its corresponding eigenvector are strictly positive due to Perron–Frobenius theorem. By the same procedure

[2] Recall that a square matrix A is Metzler if all its off-diagonal elements are nonnegative and it is irreducible if additionally its associated graph is connected (Bullo, 2019).

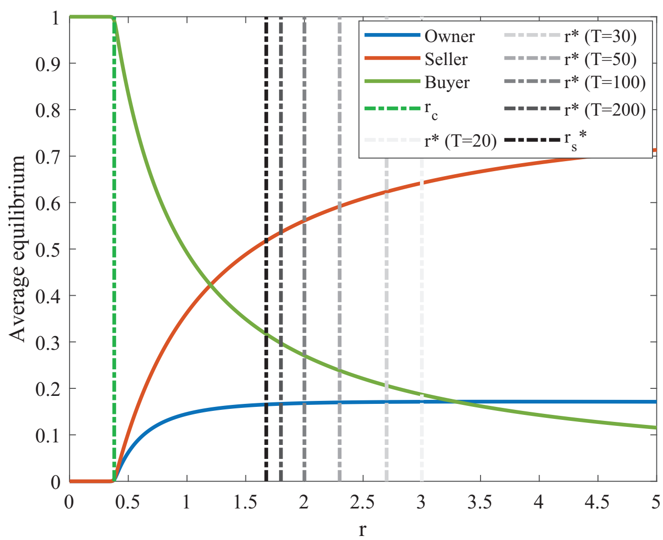

Fig. 9. Optimum incentive value for different time periods.

in the proof of Proposition 1, we can conclude the following proposition for the heterogeneous incentives:

Proposition 3. *Consider the N-intertwined model (24), or (25). If $\lambda_1(\mathbb{A}) \leq -\epsilon,\ \epsilon > 0$, where*

$$\mathbb{A} = \begin{bmatrix} \beta_1 A - \delta_1 I & \beta_2 A + \delta_2 I \\ \beta_1 RA & \beta_2 RA - \delta_2 I \end{bmatrix} \tag{28}$$

then an initial condition $[p^T(0)\, q^T(0)]^T \in [0, 1]^{2N}$ will converge to zero exponentially fast.

For further results on stability of trade-free equilibrium, we consider the regular splitting of a real Metzler matrix M as $M = \Delta + W$ where Δ is Metzler stable[3] and $W \geq 0$ is a nonnegative matrix (Fall et al., 2007, Definition 2.2). According to Fall et al. (2007, Proposition 2.1), if $M = \Delta + W$ is a regular splitting of M, then M is Metzler stable if and only if $\rho\left(-W\Delta^{-1}\right) < 1$.

Lemma 4. *The trivial equilibrium of the N-intertwined BOSB model (24), or (25), is globally exponentially stable if and only if $\rho\left(-W\Delta^{-1}\right) < 1$, where*

$$W = \begin{bmatrix} \beta_1 A & \beta_2 A \\ \beta_1 RA & \beta_2 RA \end{bmatrix}, \quad \Delta = \begin{bmatrix} -\delta_1 I & \delta_2 I \\ 0 & -\delta_2 I \end{bmatrix}$$

Proof of Lemma 4. See A.8. □

Theorem 3. *The trivial equilibrium of the N-intertwined BOSB model (24), or (25), is globally exponentially stable if and only if $\lambda_1(\mathcal{R}A) \leq 1$, or $\mathcal{R}_0 \leq 1$.*

Proof of Theorem 3. See A.9. □

The endemic equilibrium condition is attained by setting $\dot{p} = \dot{q} = 0$ in (25) as:

$$\bar{p} = [\mathrm{diag}(1 + a_i \mathcal{R}_i (A\bar{p})_i)]^{-1} \mathcal{R} A \bar{p}$$

$$\bar{q} = \frac{\delta_1}{\delta_2}(I + R)^{-1} R \bar{p} \tag{29}$$

where $a_i = \frac{\delta_1 r_i + \delta_2 (r_i + 1)}{\delta_2 (r_i + 1)} > 1$. Similar to Lemma 1, any endemic equilibrium is strongly positive. We can repeat the same procedure in the proof of Lemma 3 for $\lambda_1(\mathcal{R}A) > 1$, to reach the following lemma for heterogeneous incentives.

Lemma 5. *Suppose $\mathcal{R}_0 = \lambda_1(\mathcal{R}A) > 1$. There is a unique endemic equilibrium for (25) that is strictly positive and is the solution of (29). In fact, under the initial condition $y(0)$ a scalar multiple of u_1, with u_1 being the eigenvector corresponding to $\lambda_1(\mathcal{R}A)$ and $\max_i a_i y_i(0) \leq 1 - 1/\lambda_1(\mathcal{R}A)$, the sequence,*

$$y(k+1) = F(\mathcal{R}Ay(k)) \tag{30}$$

where $\{y(k)\}_{k\in\mathbb{N}} \subset \mathbb{R}^N$, $[F(y)]_i = \frac{y_i}{1 + a_i y_i}$, and $a_i = \frac{\delta_1 r_i + \delta_2 (1 + r_i)}{\delta_2 (r_i + 1)}$, converges to the equilibrium state $\bar{p}$: $\lim_{k\to\infty} y(k) = \bar{p}$.

Similar to the Theorem 2, we have the following stability result for the endemic equilibrium of (25):

Lemma 6. *Suppose $\mathcal{R}_0 = \lambda_1(\mathcal{R}A) > 1$. Then, the endemic equilibrium of (25) is globally asymptotically stable.*

Remark 4. Using the conditions on $\lambda_1(\mathcal{R}A)$, we can obtain some criteria directly based on the incentive vector $\boldsymbol{r}$. Let r_{min} and r_{max} be the minimum and the maximum incentive given to all agents (i.e $r_{min} = \min_i r_i$ and $r_{max} = \max_i r_i$). Since $\lambda_1(\mathcal{R}A) \leq \lambda_1(\mathcal{R})\lambda_1(A)$, we can conclude that, if

$$(r_{max} + 1)\frac{\beta_1}{\delta_1} + r_{max}\frac{\beta_2}{\delta_2} < \frac{1}{\lambda_1(A)} \tag{31}$$

then, $\lambda_1(\mathcal{R}A) \leq 1$, and the trivial equilibrium of the N-intertwined BOSB model (5) is globally exponentially stable. In the same manner, since $\lambda_1(\mathcal{R}A) \geq \lambda_{min}(\mathcal{R})\lambda_1(A)$, with $\lambda_{min}(.)$ denoting the smallest eigenvalue, we can conclude if

$$(r_{min} + 1)\frac{\beta_1}{\delta_1} + r_{min}\frac{\beta_2}{\delta_2} > \frac{1}{\lambda_1(A)} \tag{32}$$

then, $\lambda_1(\mathcal{R}A) \geq 1$, and there exists a unique endemic equilibrium that is globally asymptotically stable. Moreover, we understand by (31) and (32) that for heterogeneous incentives, the reproduction number is bounded as

$$\left[(r_{min} + 1)\frac{\beta_1}{\delta_1} + r_{min}\frac{\beta_2}{\delta_2}\right]\lambda_1(A)$$
$$\leq \mathcal{R}_0 \leq \left[(r_{max} + 1)\frac{\beta_1}{\delta_1} + r_{max}\frac{\beta_2}{\delta_2}\right]\lambda_1(A) \tag{33}$$

Remark 4 indicates that, to destabilize the trade-free equilibrium, the maximum incentive given is required to be lower-bounded by the critical incentive (11) as $r_{max} \geq r_c$. On the other hand, the condition $r_{min} \geq r_c$ assures the existence and stability of an endemic equilibrium. Thus, if all incentives are less than the critical incentive r_c the trade-free equilibrium is globally exponentially stable, and when all incentives are larger than the critical incentive r_c there is a unique endemic equilibrium that is globally asymptotically stable. However, these are conservative results in that we have still no explicit finding about the intermediate situation where some incentives are less than and some others are larger than r_c, $r_{min} \leq r_c \leq r_{max}$. We have the tight explicit results of Theorem 3 and Lemma 6 that demonstrate if R is such that $\lambda_1(\mathcal{R}A) \leq 1$ the origin is exponentially stable, and if $\lambda_1(\mathcal{R}A) > 1$ there is a unique asymptotically stable endemic equilibrium. However, these criteria yield no explicit result directly based on individual incentives r_i. For more explicit criterion, we may attain further conditions based on a factor other than maximum or minimum incentive; e.g. based on average incentive. In an attempt to achieve some criterion based on the average incentive, we pose the following Lemma 7. First, let us consider the incentive vector $\boldsymbol{r} = r_{ave} + \tilde{r}$ where r_{ave} denotes the average of components of $\boldsymbol{r}$ and $\tilde{r}$ denotes the deviation from the mean value r_{ave}, and consider $\tilde{R} = \mathrm{diag}(\tilde{r})$.

[3] i.e. Δ is Metzler with negative eigenvalues real parts (Fall et al., 2007).

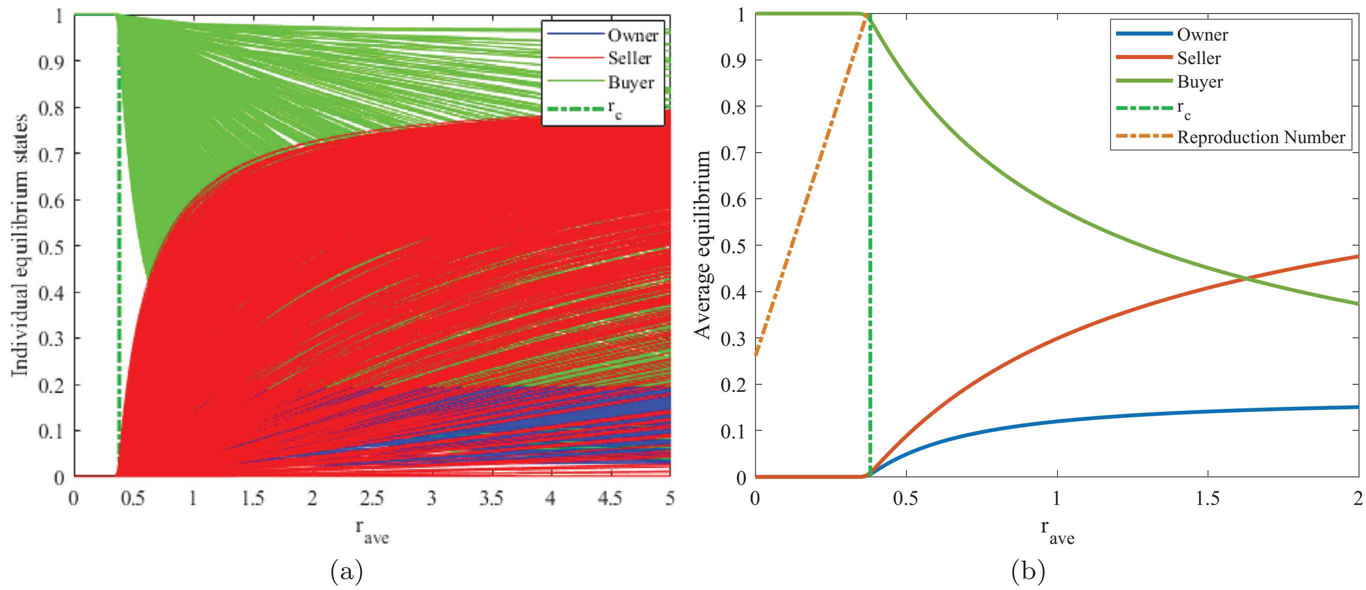

Fig. 10. (a) Individual, and (b) average, equilibrium states with heterogeneous incentive values.

Lemma 7. *Let $\bar{A}$ be defined with replacing $r = r_{ave}$ in (8) and suppose the incentive $r = r_{ave}$ satisfies (10), so that $r_{ave} < r_c$. Then the trivial equilibrium of the N-intertwined BOSB model (5) is globally exponentially stable when the maximum deviation $\tilde{r}_{max} = \max \tilde{r} > 0$ from the average value is such that*

$$\tilde{r}_{max} < \frac{\epsilon}{2\beta_2\lambda_1(A)} \le \frac{-\lambda_1(\bar{A})}{2\beta_2\lambda_1(A)}.$$

Proof of Lemma 7. See A.10 □

Remark 5. The importance of Lemma 7 is establishing a lower-bound for deviation from the average incentive in order to destabilize the origin and have a stable endemic equilibrium. Therefore, when the average incentive r_{ave} is less than the critical value r_c in (11), the standard deviation of incentive assignment should be large enough to have a stable endemic equilibrium and active trading.

Fig. 10 shows the equilibrium of the BOSB with heterogeneous incentives for different values of average incentive factor r_{ave} in an Erdos–Renyi graph with 1000 nodes. Here, we have randomly assigned an incentive value $0 < r_i < 3$ to each agent i, and next, have multiplied all incentives by an increasing factor starting from zero to obtain a spectrum of values for r_{ave}. As it can be observed, below the threshold $\mathcal{R}_0 = \lambda_1(\mathcal{R}A) = 1$, only the trade-free equilibrium exists, while incentive distribution leading to $\mathcal{R}_0 = \lambda_1(\mathcal{R}A) > 1$ gives birth to a unique endemic equilibrium. In addition, comparing Figs. 10a and 5a, we note that the equilibrium state for heterogeneous incentives is more distributive, i.e. the standard deviation of equilibrium states for heterogeneous incentives is higher than that in homogeneous incentive. In general, the higher the standard deviation of incentive distribution, the higher the standard deviation of equilibrium states. By Fig. 10b we also note that, the average incentive factor r_{ave} yields a good criterion for estimating the threshold in this case, although this is not the case always and the average incentive can not yield a precise criterion when the standard deviation of incentive allocation is effectively large. Here, r_c is the same as in (11).

7. Maximizing profit: heterogeneous incentive values

For heterogeneous incentive values, the profit function over time period T is defined as

$$\Pi(\boldsymbol{r}) = \Pi_0 \sum_i n^i_{B\to O} + \sum_i (\Pi_0 - f(r_i)) n^i_{B\to S} \tag{34}$$

where $n^i_{B\to O} = n^i_{B\to O}(T)$ and $n^i_{B\to S} = n^i_{B\to S}(T)$ are the number of transitions from states B to O and S, respectively, for an individual i during the time interval T. The expected profit is computed as

$$\mathrm{E}[\Pi(\boldsymbol{r})] = \Pi_0 \sum_i \mathrm{E}\left[n^i_{B\to O}\right] + \sum_i (\Pi_0 - f(r_i))\mathrm{E}\left[n^i_{B\to S}\right] \tag{35}$$

where

$$\begin{aligned}\mathrm{E}\left[n^i_{B\to O}\right] &= \frac{1}{r_i}\mathrm{E}\left[n^i_{B\to S}\right]\\ &= \int_0^T (1 - p_i - q_i)\left(\beta_1 \sum_j a_{ij} p_j + \beta_2 \sum_j a_{ij} q_j\right) dt\end{aligned} \tag{36}$$

With $\mathrm{E}[n^i_{B\to S}] = r_i \mathrm{E}[n^i_{B\to O}]$, the profit is written as $\mathrm{E}[\Pi(\boldsymbol{r})] = \sum_i(\Pi_0(r_i+1) - r_i f(r_i))\mathrm{E}[n^i_{B\to O}]$. By repeating the same procedure performed to reach (23), that is by using (36) to obtain the transition $\mathrm{E}[n^i_{B\to O}]$ at each time step Δt as $(1 - p_i - q_i)(\beta_1 \sum_j a_{ij} p_j + \beta_2 \sum_j a_{ij} q_j)\Delta t$ and inserting the equilibrium condition (29), the profit at each time step of the steady state can be calculated as $\delta_1[\Pi_0 \boldsymbol{1}^T - \boldsymbol{r}^T \mathrm{diag}([\frac{f(r_i)}{r_i+1}])]\bar{p}\Delta t$. The following constrained nonlinear programming is then established to maximize the steady state profit:

$$\max_{\boldsymbol{r},\bar{p}} \quad \left[\Pi_0 \boldsymbol{1}^T - \boldsymbol{r}^T \mathrm{diag}\left(\left[\frac{f(r_i)}{r_i+1}\right]\right)\right]\bar{p}$$

$$\text{s.t.} \begin{cases} [\mathrm{diag}(1 + a_i \mathcal{R}_i (A\bar{p})_i)]\bar{p} - \mathcal{R}A\bar{p} = 0 \\ \boldsymbol{r}^T \boldsymbol{1} \le c \\ \boldsymbol{r} \ge 0 \end{cases} \tag{37}$$

where the total incentive given to all individuals is supposed to be upper-bounded by the constant c. The case where there is no

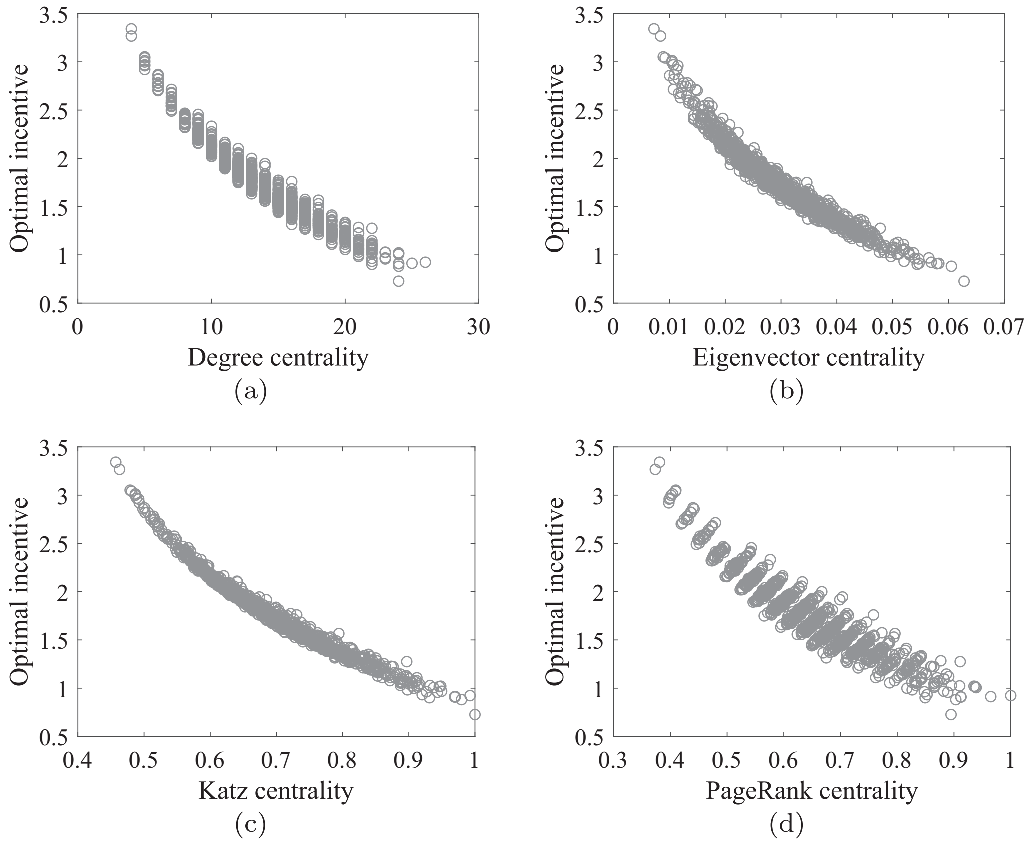

Fig. 11. Optimal incentives for different centrality measures when the total incentive is not limited ($\boldsymbol{c = \infty}$) (a) Node degree. (b) Eigenvector centrality. (c) Katz centrality. (d) PageRank centrality.

constraint on the total incentive is equivalent to $c = \infty$. We can conclude that the nonlinear programming (37) holds a unique optimal solution by using Lemma 6 to assure that the feasible set of the optimization problem is nonempty, and by assuming $f(r_i)$ is such that $r_i/(r_i+1)f(r_i)$ is convex for $r_i > 0$.

We solve the nonlinear programming (37) for an Erdos–Renyi network with 1000 nodes using the SQP (Nocedal & Wright, 2006). Fig. 11 shows scatter plots of optimal incentives versus some common centrality measures (Liao et al., 2017), when there is no restriction on the total incentive c. As a general pattern, it can be observed in Fig. 11 that less central nodes receive more incentives. This observation indicates that when there is no limit on the incentive amount, the optimal strategy strengthens the externality's effect on less central nodes by increasing their incentives. In such conditions of no restriction on optimal incentives, externalities' effect on most central nodes is essentially due to the number of their owner and seller neighbors. In spite of the general pattern observed in Fig. 11, not all less central individuals receive larger incentives. This indicates that although there is a strong correlation between centrality and incentive allocation, there is no trivial law to achieve the optimal incentives absolutely based on usual centrality measures.

In Fig. 12, we show scatter plots of optimal incentives versus eigenvector centrality for different values of total incentive c. We do not show other centrality measures due to qualitatively similar results (as implied by Fig. 11). When the total incentive budget c is very limited, as in Figs. 12a and b, the optimal incentive allocation holds a completely unbalanced pattern. While the majority of individuals receives no incentive, some very few others, mostly nodes with highest centrality, receive large amounts. This observation can be explained by recalling Lemma 7, which suggests when the average incentive is below the critical value, large standard deviation of incentive distribution is needed to have a stable endemic equilibrium. In fact, the average incentives in Figs. 12a and b are $r_{ave} = 0.25$ and $r_{ave} = 0.1$, respectively, which are less than the critical value $r_c = 0.3803$ computed by (11). Therefore, based on Lemma 7, the optimal mechanism in each case leads to a high standard deviation in incentive allocation for reaching a stable endemic equilibrium. Examining the reproduction numbers, we have $\mathcal{R}_0 = \lambda_1(\mathcal{R}A) = 1.5746$ in Fig. 12a, and $\mathcal{R}_0 = \lambda_1(\mathcal{R}A) = 1.6668$ in Fig. 12b. Hence, both cases result in reproduction numbers greater than 1 and stable endemic equilibria, despite having average incentives significantly smaller than the critical incentive r_c. In general, when the incentive budget is tight, the incentive to consumers with the least centralities is effectively wasted since these individuals have little chance to influence the whole network with limited resources. Instead, the less central nodes are influenced by their central neighbors. This situation continues by increasing the total incentive to $c = 500$ and $c = 750$, the cases shown in Figs. 12c and d, respectively, where the number of more central nodes receiving incentive increases while the least central nodes still receiving no incentive. For the larger total incentive $c = 1000$ in Fig. 12e, we note there is no nodes receiving no incentive and almost all nodes receive incentive, with nodes of larger centralities still receiving larger incentive.

This implies that, when there is a limited total incentive, the optimal incentive determination mechanism prioritizes and assigns more incentive to central individuals since they can produce larger externalities effect on the whole network even with limited resources. Therefore, when the total incentive is limited, the tradeoff between the exploitation and the influence (Bloch & Quérou, 2013) is in favor of influence, so that the monopolist promotes the good

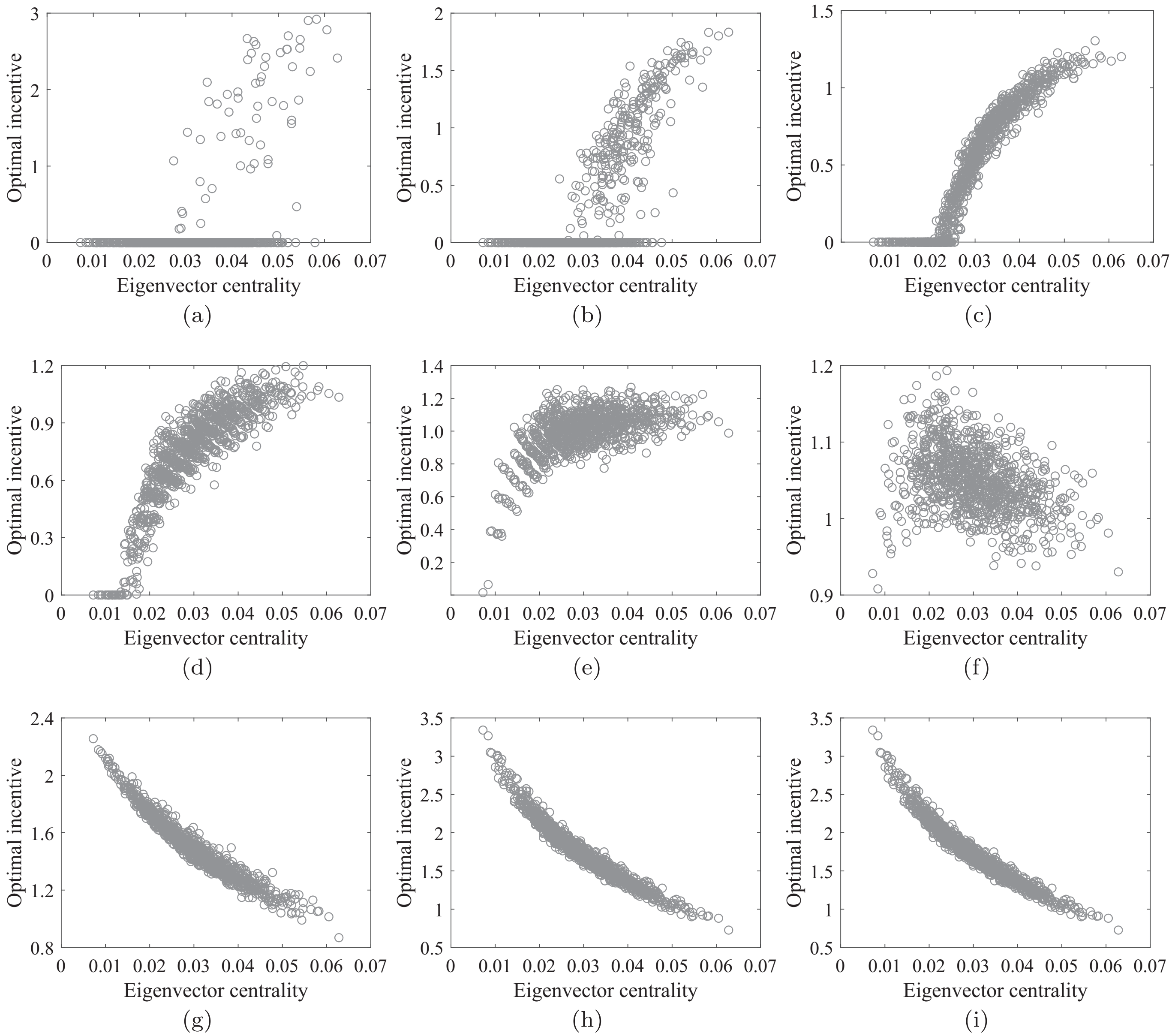

Fig. 12. Optimal incentives versus eigenvector centrality when (a) $\boldsymbol{c} = \mathbf{100}$, (b) $\boldsymbol{c} = \mathbf{250}$, (c) $\boldsymbol{c} = \mathbf{500}$, (d) $\boldsymbol{c} = \mathbf{750}$, (e) $\boldsymbol{c} = \mathbf{1000}$, (f) $\boldsymbol{c} = \mathbf{1200}$, (g) $\boldsymbol{c} = \mathbf{1500}$, (h) $\boldsymbol{c} = \mathbf{2000}$, (i) the total incentive is not limited $(\boldsymbol{c} = \infty)$.

through more central consumers in order to maximize influence over neighboring nodes. Some similar results have been reported in optimal resource allocation for containing disease spreading (Preciado, Zargham, Enyioha, Jadbabaie, & Pappas, 2014) where for limited resources the nodes with larger centralities are assigned most of available budget.

However, the situation changes and the system dynamics bifurcates as the incentive budget c increases further. First, Fig. 12f indicates that, when $c = 1200$, there is almost no regular pattern for incentive allocation, and it is neither increasing nor decreasing with individuals centrality. With Figs. 12g, h, and i, we observe a completely different pattern where, given an unrestricted or a large available total incentive, there are no individuals receiving no incentive, while less central nodes commonly receiving larger incentive amounts. In such conditions, i.e. when the total incentive is not significantly limited, the tradeoff between exploitation and influence is resolved in favor of exploitation of more central consumers, so that these nodes are charged higher prices in order to exploit their higher degree of influence. In this case, the less central nodes are stimulated by receiving larger incentive amounts, and not by influence of their central neighbors. This observed dynamic sheds light on a long standing dispute in the TSS literature as to whether more central individuals should be selected as initiators of a viral campaign. While there are contradicting points of view on this issue (Christophe, Wuyts, Dekimpe, Gijsbrechts, & Pieters, 2010; Cohen & Harsha, 2019; Hinz et al., 2011; Iyengar & Lepper, 2000; Van der Lans et al., 2010; Watts & Dodds, 2007), our results show that under different incentive budgets, relying on more central individuals may or may not be the best strategy.

Finally, Fig. 13 shows the maximum expected profit attainable at each instant of steady state for different total incentives c. As illustrated in Fig. 13, the maximum profit is a monotonically increasing function of incentive budget c and approaches a fixed value as c increases.

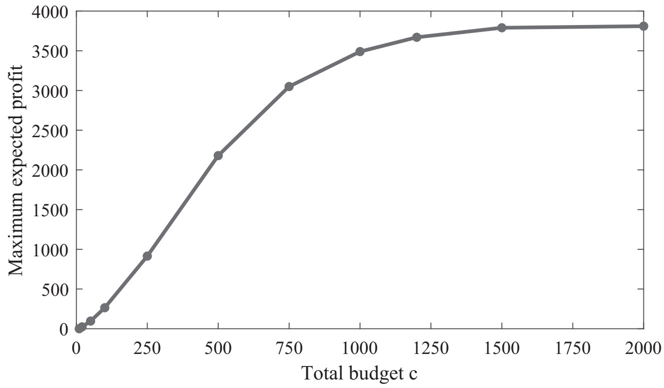

Fig. 13. Maximum expected profit attainable at each instant of steady state for different total incentives c.

8. Managerial implications

This study has three key takeaways for practitioners and managers. First, a low incentive rate may not have a sustainable effect on sales. Our model revealed that the incentive values that fall below a threshold might not be encouraging enough to keep the consumers trading, and thus, the sales eventually might vanish (i.e., trade-free equilibrium). Second, it was found that if the monopolist is willing to reward every consumer equally (i.e., homogenous incentives), there is a unique optimum incentive rate that maximizes the profit and whose value decreases as the planning time horizon increases. This finding led to an optimal strategy in designing the homogenous incentive rates, which tends to begin with a maximum permissible incentive value for optimal profit in a short time horizon and gradually decreases it to a value that maximizes the profit in an infinite time horizon (i.e., endemic equilibrium). A third takeaway pertains to the case where a firm rewards each individual differently (i.e., heterogenous incentives). While our intuition may induce an incentive allocation based on the individuals' centrality, we observed that different centrality measurements could not trivially determine the optimal incentive allocation, although some strong correlation exists between centrality measures and incentive allocation. Indeed, our model explicated that there is no straightforward incentive rate determination strategy in a heterogeneous incentive scenario. However, there seems to be a relationship between the individuals' measure of centrality and the optimum reward they receive upon generating sales. The centrality of a node can affect the optimal incentive rate in two different countervailing manners. On the one hand, a more central node generates more positive externalities on its neighbors and hence, should be incentivized more. On the other hand, more central individuals have more opportunities to generate sales, and if they receive a larger incentive, they can negatively impact the monopolist's profit. Thus, a monopolist may choose to price discriminate by trading off "influence" and "exploitation" (Bloch & Quérou, 2013). This tradeoff either leads to higher incentive rates at more central nodes to maximize influence over neighboring nodes or to lower incentive rates at more central nodes to exploit the higher valuation of more central consumers.

Similarly, our findings show that the optimal incentive allocation makes a tradeoff between lowering the incentive at more central nodes to exploit the nodes centrality or raising the incentive at more central nodes to maximize influence on other consumers. When the total incentive is not limited or is loosely limited, the tradeoff between influence and exploitation is resolved in favor of exploitation, and more central nodes are given smaller incentives. In such a condition, the less central nodes are stimulated by offering more substantial incentives, instead of being influenced by their central neighbors. On the other hand, when the total incentive is moderately or tightly limited, our findings show that the tradeoff favors the influence by offering the more central nodes larger incentives so that they influence the less central nodes, which in turn receives very small or zero incentives. Finally, we recall that our results are limited to undirected graphs, and they may change when our approach is examined on directed graphs. Some implications may be observed from Candogan et al. (2012), where the authors investigate a two-stage pricing-consumption game model and show that, when the underlying network is directed, the agents that are offered the most favorable prices are the ones that influence highly central agents.

9. Conclusion

In this paper, we have established a new model of viral marketing for a monopolist selling a single good under network externalities. In our so called BOSB model, the individuals interact with each other while assuming three possible roles of potential buyers, owners, or sellers. A potential buyer can become a seller by promoting the good to his neighbors while collecting a reward (i.e., incentive) for the sales she generates. The state of an individual depends on the state of his neighbors over the network. By constructing different transition probabilities, we developed an N-intertwined model that is the mean field approximation of the corresponding continuous-time Markov process. We investigated two cases of homogeneous and heterogeneous incentive values. In each case, by studying the spectra of the developed model, we established the existence and stability conditions of trade-free and endemic equilibrium states and expressed different criteria in terms of the epidemic reproduction number. We have also suggested two convergent sequences to compute the unique endemic equilibria for homogeneous and heterogeneous cases.

Taking the incentive as a control parameter, we investigated the optimal incentive rate determination problem to achieve maximum profit. To this end, we determined the optimal homogeneous incentive and the optimal heterogeneous incentive allocation through the proposed corresponding nonlinear programmings. In the case of homogeneous incentive, the optimal incentive rate is such that a tradeoff is made between the number of transitions from the potential buyer state to each of the owner and seller states. While raising the incentive rate increases the monopolist profit through shifting individuals to the owner and seller states, an excessive incentive rate can inadvertently lessen the profit by encouraging more individuals to stay in the seller state and hence, fewer transitions from potential buyers to owners. The situation is more involved in the case of heterogeneous incentives where more central individuals are favored more when the incentivization budget is tight, and conversely, less central nodes are rewarded more generously when the incentivization budget is abundant.

In the context of viral marketing, one is typically interested in amplifying the spread process through an incentivization schema. However, the methods proposed in this paper can likewise be applied to the scenarios where a spreading process is to be contained. One such process is encountered in epidemiology, where the spread of a virus needs to be restrained. For this purpose, the incentive rate r can be repurposed to represent the cost of protecting an individual against receiving or passing a virus to others. Investigating homogeneous and heterogeneous protection costs and their effect on the virus spread process can be a fruitful application of the presented methods in this study.

A natural direction to extend this study is to consider incentive determination in a competitive environment. In the simplest case, when only two firms compete over the sales of a particular good, a model such as the competitive epidemic spreading studied by Sahneh and Scoglio (2013) can be considered and extended under viral marketing setting. The problem becomes more interesting when the competition occurs in a multilayer network where network layers represent the distinct transmission routes of the information. Then, characterizing the existence/coexistence conditions of different goods and the IRD problem as functions of various network layers structures will be a challenging problem whose solution can establish meaningful results. Moreover, since our results are limited to undirected graphs, we can use more recently developed approaches, such as the one considered in Khanafer et al. (2016), to explore how our results may change when examined on directed graphs and extend our work. Another interesting subject for future work is time-varying incentive determination and the corresponding dynamic optimization. The analyses of the model considered in this paper, and the associated static optimizations are based on the assumption that the incentive amount given to each individual is constant. To extend the obtained results, optimal time-varying incentive (Ajorlou et al., 2016) determination can be considered and resolved in the framework of optimal control (Lorch et al., 2018) or model predictive control (MPC) (Watkins, Nowzari, & Pappas, 2018). Furthermore, the power of more recently developed data-driven and machine learning approaches (Brunton & Kutz, 2019) in the identification and control of complex systems seems promising when studying dynamical phenomena over complex networks. Therefore, their application to dynamic incentive determination is expected to yield significant results.

Appendix A. Proofs

A.1. Proof of Proposition 1

We first note from (6) that

$$\begin{bmatrix}\dot{p}\\ \dot{q}\end{bmatrix} = \begin{bmatrix}\beta_1 A - \delta_1 I & \beta_2 A + \delta_2 I\\ r\beta_1 A & r\beta_2 A - \delta_2 I\end{bmatrix}\begin{bmatrix}p\\ q\end{bmatrix} - \mathcal{H}(p,q)$$
$$= \mathcal{A}\begin{bmatrix}p\\ q\end{bmatrix} - \mathcal{H}(p,q) \tag{A.1}$$

where

$$\mathcal{H}(p,q) = \begin{bmatrix}(P+Q)(\beta_1 Ap + \beta_2 Aq)\\ r(P+Q)(\beta_1 Ap + \beta_2 Aq)\end{bmatrix} \geq 0 \tag{A.2}$$

for $p,\ q \geq 0$. Now, consider the Lyapunov candidate $V(t) = 1/2x^T x$, $x = \left[p^T q^T\right]^T$. By (A.1), we have

$$\dot{V} = x^T \mathcal{A} x - x^T \mathcal{H} \leq x^T \mathcal{A} x \leq -\epsilon \|x\|^2$$

where the first inequality follows from $\mathcal{H}(p,q) \geq 0$ and the fact that $x = [p^T q^T]^T$ is trapped in the positive compact set $[0,\ 1]^{2N}$.

A.2. Proof of Proposition 2

If λ is an eigenvalue of $\mathcal{A}$, then $\mathcal{A}\begin{bmatrix}u\\ v\end{bmatrix} = \lambda\begin{bmatrix}u\\ v\end{bmatrix}$, with the corresponding eigenvector $\begin{bmatrix}u\\ v\end{bmatrix} \in \mathbb{R}^{2N\times 1}$. Upon (8), we have

$$\begin{cases}(\beta_1 A - \delta_1 I)u + (\beta_2 A + \delta_2 I)v = \lambda u\\ r\beta_1 Au + (r\beta_2 A - \delta_2 I)v = \lambda v\end{cases} \tag{A.3}$$

Multiplying the first equality in (A.3) by r and subtracting the result from the second equality, it follows:

$$u = \frac{\lambda + (r+1)\delta_2}{r(\delta_1 + \lambda)} v \tag{A.4}$$

Inserting (A.4) in the second of (A.3), we get

$$(\gamma A - \delta_2 I)v = \lambda v \tag{A.5}$$

with $\gamma = \frac{(\beta_1 + r\beta_2)\lambda + (r+1)\beta_1\delta_2 + r\delta_1\beta_2}{\delta_1 + \lambda}$. Dividing both sides of (A.5) by γ it follows that $\frac{\lambda}{\gamma}$ is an eigenvalue of $A - \delta_2 I$. Recall that $\lambda(A - \frac{\delta_2}{\gamma}I) = \lambda(A) - \frac{\delta_2}{\gamma}$. Then, dividing (A.5) by γ yields $\lambda(A) - \frac{\delta_2}{\gamma} = \frac{\lambda(\mathcal{A})}{\gamma}$. On inserting γ as defined after Eq. (A.5), we conclude the following second order algebraic equation for $\lambda(\mathcal{A})$:

$$\lambda^2(\mathcal{A}) + (a+b)\lambda(\mathcal{A}) + ab - c = 0 \tag{A.6}$$

where $a = \delta_1 - \beta_1\lambda(A)$, $b = \delta_2 - r\beta_2\lambda(A)$, and $c = r\beta_1[\delta_2 + \beta_2\lambda(A)]\lambda(A)$. The solution of (A.6) is given by (9).

A.3. Proof of Theorem 1

With Inequality (7), it is sufficient to show that all eigenvalues of $\mathcal{A}$ are negative. Of $2N$ eigenvalues computed by (9), N eigenvalues are always negative. The remaining N eigenvalues become negative if

$$[\delta_1 + \delta_2 - (\beta_1 + r\beta_2)\lambda(A)]^2$$
$$> [(\delta_1 - \delta_2) - (\beta_1 - r\beta_2)\lambda(A)]^2 + 4r\beta_1[\delta_2 + \beta_2\lambda(A)]\lambda(A) \tag{A.7}$$

By canceling common terms in (A.7), we get

$$\delta_1\delta_2 > (1+r)\beta_1\delta_2\lambda(A) + r\beta_2\delta_1\lambda(A)$$

which can be divided by $\delta_1\delta_2\lambda(A)$ to yield

$$(r+1)\tfrac{\beta_1}{\delta_1} + r\tfrac{\beta_2}{\delta_2} < \tfrac{1}{\lambda(A)} \tag{A.8}$$

Now if (A.8) is satisfied for the maximum eigenvalue of A, we can be sure that it is satisfied for all other eigenvalues.

A.4. Proof of Lemma 1

Suppose there exists a node j in the neighbor of node i with nonzero owner probability, so that $a_{ij} = 1$ and $\bar{p}_j > 0$. Then, examining the ith row of (15), it is observed that $\bar{p}_i > 0$ and by (14) $\bar{q}_i > 0$. This procedure can be repeated for the nodes in the neighbor of i, and so on. Hence, if the contact network is connected and at least one of the agents have nonzero owner (or seller) probability, then $\bar{p}_i, \bar{q}_i > 0$ for all $i \in \{1, \ldots, N\}$.

Please cite this article as: A. Tavasoli, H. Shakeri and E. Ardjmand et al., Incentive rate determination in viral marketing, European Journal of Operational Research, https://doi.org/10.1016/j.ejor.2020.07.046

A.5. Proof of Lemma 2

We note by (15) and the first of (16) that $[\frac{\beta_1}{\delta_1}(r+1)+r\frac{\beta_2}{\delta_2}]^{-1}\bar{p}\ll A\bar{p}$. From (12), we have $\bar{p}\ll\frac{\mathcal{R}_0}{\lambda_1(A)}A\bar{p}$. Then, the inner product of both sides of this inequality by $\bar{p}$, with using the fact that $\bar{p}^TA\bar{p}\le\lambda_1(A)\|\bar{p}\|^2$, indicates $\|\bar{p}\|^2<\frac{\mathcal{R}_0}{\lambda_1(A)}\bar{p}^TA\bar{p}\le\mathcal{R}_0\|\bar{p}\|^2$, which proves the lemma.

A.6. Proof of Lemma 3

The proof is based on the approach utilized in the proof by Mei et al. (2017, Theorem 4.3). We first investigate the existence problem. Consider the monotonically-increasing function $f(y)=\frac{y}{1+ay}$ for $y\in\mathbb{R}_{\ge}0$. For vector variables $y\in\mathbb{R}^N_{\ge 0}$, let $F(y)=(f(y_1),\dots,f(y_N))$. Observe that $\bar{p}$ is an equilibrium if and only if $F(\frac{\mathcal{R}_0}{\lambda_1}A\bar{p})=\bar{p}$. That is, $\bar{p}$ is an equilibrium if and only if it is a fixed point of $\mathcal{F}$, where $\mathcal{F}(\bar{p})=F(\frac{\mathcal{R}_0}{\lambda_1}A\bar{p})$. It is noted that $F(\frac{\mathcal{R}_0}{\lambda_1}Ay)\gg F(\frac{\mathcal{R}_0}{\lambda_1}Az)$ when $y\gg z\ge\mathbf{0}$. This is due to the facts that f is monotonically increasing and also the contacting graph is connected so that $Ay\gg Az$. Moreover, for any $\sigma>1$ and $y>0$, we have $f(\sigma y)\ge y$ if and only if $ay\le 1-1/\sigma$. Now, consider the sequence $\{y(k)\}_{k\in\mathbb{N}}\subset\mathbb{R}^N$ by $y(k+1)=\mathcal{F}(y(k))=F(\frac{\mathcal{R}_0}{\lambda_1}Ay(k))$. Let u_1 be the eigenvector of A corresponding to the largest eigenvalue λ_1, so $Au_1=\lambda_1u_1$, and suppose $y(0)\ge\mathbf{0}$ is a scalar multiple of u_1 with $a\max_i y_i(0)\le 1-1/\mathcal{R}_0$. Then, $F(\frac{\mathcal{R}_0}{\lambda_1}Ay(0))_i=F(\mathcal{R}_0y_i(0))\ge y_i(0)$. This implies $y(1)\ge y(0)$, which in turn shows $y(2)=F(\frac{\mathcal{R}_0}{\lambda_1}Ay(1))\ge F(\frac{\mathcal{R}_0}{\lambda_1}Ay(0))=y(1)$, where the inequality results since f is monotonically increasing. By induction, $y(k+1)\ge y(k)$. Therefore, the sequence $\{y(k)\}$ is monotonically nondecreasing and entry-wise upper-bounded by $\mathbf{1}$. Then, we conclude, by the fundamental Bolzano–Weierstrass theorem, that the sequence $\{y(k)\}$ is convergent. Therefore, $y(k)$ converges to some $\mathbf{0}\ll\bar{p}\ll\mathbf{1}$ such that $F(\frac{\mathcal{R}_0}{\lambda_1}A\bar{p})=\bar{p}$.

We next show the uniqueness of the endemic equilibrium. To do so, assume, by contradiction, that $\bar{p}$ and $\bar{s}$ are two distinct equilibriums. We know from Lemma 1 that $\bar{p},\bar{s}\gg\mathbf{0}$. Let $\alpha=\min_j\{\bar{s}_j/\bar{p}_j\}$, and assume without loss of generality that $\alpha<1$. Determine i as $\alpha=\bar{s}_i/\bar{p}_i$. Then $\bar{s}\ge\alpha\bar{p}$ and $\bar{s}_i=\alpha\bar{p}_i$. We now write

$$\begin{aligned}\left[F\left(\frac{\mathcal{R}_0}{\lambda_1}A\bar{s}\right)-\bar{s}\right]_i&=f\left(\frac{\mathcal{R}_0}{\lambda_1}(A\bar{s})_i\right)-\alpha\bar{p}_i\\&\ge f\left(\frac{\alpha\mathcal{R}_0}{\lambda_1}(A\bar{p})_i\right)-\alpha\bar{p}_i\\&>\alpha f\left(\frac{\mathcal{R}_0}{\lambda_1}(A\bar{p})_i\right)-\alpha\bar{p}_i\\&=\alpha\left[F\left(\frac{\mathcal{R}_0}{\lambda_1}A\bar{p}\right)-\bar{p}\right]_i=0\end{aligned}\tag{A.9}$$

where to write the two inequality relations we have considered the facts that f is monotonically increasing, the contacting graph is connected, and $0<\alpha<1$, and the last equality results because $\bar{p}$ is an equilibrium. In fact, in the second inequality we have considered $f(\alpha y)>\alpha f(y)$, since $\frac{\alpha y}{(1+a\alpha y)}>\frac{\alpha y}{(1+ay)}$, for $0<\alpha<1$ and $y\in\mathbb{R}_{>0}$. Therefore, $[F(\frac{\mathcal{R}_0}{\lambda_1}A\bar{s})-\bar{s}]_i>0$ and this contradicts $\bar{s}$ being an equilibrium. The uniqueness of the endemic equilibrium is readily a result of monotonically-increasing function f. In fact, any monotonically-increasing function $f(x)$, with $f(0)=0$, can intersect the line $y=x$ at most at one nonzero point.

A.7. Proof of Theorem 2

We follow the procedure utilized in the proof by (Khanafer et al., 2016, Theorem 2), motivated by the properties of positive systems concept (Bullo, 2018; Fall et al., 2007; Farina & Rinaldi, 2011; Mei et al., 2017). We first write the model (6) in the following form:

$$\dot{x}=[-D+(I-\mathrm{diag}(Jx))B]x\tag{A.10}$$

where $x=\begin{bmatrix}p\\q\end{bmatrix}$, $-D=\begin{bmatrix}-\delta_1I&\delta_2I\\0&-\delta_2I\end{bmatrix}$, $B=\begin{bmatrix}\beta_1A&\beta_2A\\r\beta_1A&r\beta_2A\end{bmatrix}$, $J=\begin{bmatrix}I&I\\I&I\end{bmatrix}$. So, the equilibrium point $\bar{x}=\begin{bmatrix}\bar{p}^T&\bar{q}^T\end{bmatrix}^T$ satisfies

$$[-D+(I-\mathrm{diag}(J\bar{x}))B]\bar{x}=0\tag{A.11}$$

Consider the error function $X=x-\bar{x}$, and note by (A.10) and (A.11) that

$$\dot{X}=[-D+(I-\mathrm{diag}(J\bar{x}))B]X-\mathrm{diag}(Bx)JX\tag{A.12}$$

Consider the matrix $\Lambda(\bar{x})=-D+(I-\mathrm{diag}(J\bar{x}))B$. We note that $\Lambda(\bar{x})$ is a Metzler matrix since its off-diagonal entries are nonnegative; $B(i,j)\ge 0,\forall i\ne j$. In addition, since the underlying graph is connected, $\Lambda(\bar{x})$ is also irreducible, i.e. there exists no permutation matrix T such that $T^T\Lambda(\bar{x})T$ is block triangular (note that we can check a matrix $M_{n\times n}$ is irreducible by verifying that for all partitions $\{\mathcal{I},\mathcal{J}\}$ of the index set $\{1,\dots,n\}$ there exist $i\in\mathcal{I}$ and $j\in\mathcal{J}$ such that $M_{ij}\ne 0$ (Bullo, 2018)). Eq. (A.11) indicates that, for $\mathcal{R}_0>1$, there exists the endemic equilibrium $\bar{x}\gg 0$ such that $\Lambda(\bar{x})\bar{x}=0$. Since $\bar{x}$ is strictly positive, the Perron–Frobenius theorem for Metzler irreducible matrices (Farina and Rinaldi, 2011, Theorem 17) shows that $\mu(\Lambda(\bar{x}))=0$, where the stability modulus $\mu(.)$ denotes the largest real part in the eigenvalue set of the corresponding matrix. Then, it follows from (Khanafer et al., 2016, Lemma A.1) that there exists a positive diagonal matrix K such that $\Lambda(\bar{x})^TK+K\Lambda(\bar{x})$ is negative semidefinite. Consider the Lyapunov function $V(X)=X^TKX$. Then, the time derivative of $V(X)$ along (A.12) becomes

$$\begin{aligned}\dot{V}&=X^T\left[\Lambda(\bar{x})^TK+K\Lambda(\bar{x})\right]X-2X^TK\mathrm{diag}(Bx)JX\\&\le-2X^TK\mathrm{diag}(Bx)JX\le 0\end{aligned}\tag{A.13}$$

where the first inequality results because $\Lambda(\bar{x})^TK+K\Lambda(\bar{x})$ is negative semidefinite, and the second inequality is due to the fact that the matrix $K\mathrm{diag}(Bx)J$ is positive semidefinite. In fact, we note that $K\mathrm{diag}(Bx)$ is diagonal with positive diagonal entries for $x\gg 0$, and that, for any positive definite diagonal matrix $M=\mathrm{diag}([M_1,\dots,M_{2N}])$, the matrix MJ is positive semidefinite with N eigenvalues identically zero and the remaining N eigenvalues $\lambda_i=M_i+M_{i+N}$. Next, following the same procedure in the proof by Khanafer et al. (2016, Theorem 2), it can be shown that $X^TK\mathrm{diag}(Bx)JX=0$ if and only if $X=0$, or $x=\bar{x}$. Therefore, the asymptotic stability of the endemic equilibrium follows from the LaSalle's invariant set principle.

A.8. Proof of Lemma 4

We note that $\mathbb{A}$ given by (28) and W are Metzler. In addition, Δ is Metzler stable, with the repeated eigenvalues $\{-\delta_1,-\delta_2\}<0$. Therefore, $\mathbb{A}=\Delta+W$ is a regular splitting of $\mathbb{A}$. The proof accordingly follows from Fall et al. (2007, Proposition 2.1).

A.9. Proof of Theorem 3

We examine the condition $\rho\left(-W\Delta^{-1}\right) < 1$. Consider the inverse matrix

$$\Delta^{-1} = \begin{bmatrix} -\frac{1}{\delta_1}I & -\frac{1}{\delta_1}I \\ 0 & -\frac{1}{\delta_2}I \end{bmatrix}.$$

Note that $\Delta^{-1}\Delta = I$. We have,

$$-W\Delta^{-1} = \begin{bmatrix} \frac{\beta_1}{\delta_1}A & \left(\frac{\beta_1}{\delta_1}+\frac{\beta_2}{\delta_2}\right)A \\ \frac{\beta_1}{\delta_1}RA & \left(\frac{\beta_1}{\delta_1}+\frac{\beta_2}{\delta_2}\right)RA \end{bmatrix}.$$

Of the $2N$ eigenvalues of $-W\Delta^{-1}$, N eigenvalues are identically zero, since the N last rows are scalar multiples of the N first rows. The eigenvalue problem for the above matrix is written as

$$\begin{cases} \frac{\beta_1}{\delta_1}Au + \left(\frac{\beta_1}{\delta_1}+\frac{\beta_2}{\delta_2}\right)Av = \lambda u \\ \frac{\beta_1}{\delta_1}RAu + \left(\frac{\beta_1}{\delta_1}+\frac{\beta_2}{\delta_2}\right)RAv = \lambda v \end{cases} \tag{A.14}$$

with λ and $\left[u^T\ v^T\right]^T$ the eigenvalue and the corresponding eigenvector of $-W\Delta^{-1}$, respectively. Summing the two equalities in (A.14) gives

$$\left[\frac{\beta_1}{\delta_1}(R+I) + \frac{\beta_2}{\delta_2}R\right]A(u+v) + \frac{\beta_2}{\delta_2}A(v-Ru) = \lambda(u+v).$$

Multiplying the first equation of (A.14) by R and subtracting from the second one, considering A is symmetric and R diagonal, we get $v - Ru = 0$ for $\lambda \neq 0$. Therefore, the above equation yields

$$\left[\frac{\beta_1}{\delta_1}(R+I) + \frac{\beta_2}{\delta_2}R\right]A(u+v) = \lambda(u+v),$$

or $\mathcal{R}A(u+v) = \lambda(u+v)$. This means, the nonzero eigenvalues of $-W\Delta^{-1}$ are the same as the eigenvalues of $\mathcal{R}A$. Hence, $\rho\left(-W\Delta^{-1}\right) < 1$ is equivalent to $\rho(\mathcal{R}A) < 1$, or by Perron–Frobenius theorem, to $\lambda_1(\mathcal{R}A) < 1$.

A.10. Proof of Lemma 7

We first rewrite the second equation of (25) as

$$\begin{aligned}\dot{q} &= r_{ave}(I-P-Q)(\beta_1Ap + \beta_2Aq) - \delta_2 q \\ &\quad + \tilde{R}(I-P-Q)(\beta_1Ap + \beta_2Aq)\end{aligned}$$

Let $\bar{\mathcal{H}} \geq 0$ be defined with replacing $r = r_{ave}$ in (A.2). Then, (25) is written as

$$\dot{x} = \bar{A}x - \bar{\mathcal{H}}(p,q) + \mathcal{K}(p,q)$$

where

$$\mathcal{K}(p,q) = \begin{bmatrix} 0 \\ \tilde{R}(I-P-Q)(\beta_1Ap+\beta_2Aq) \end{bmatrix}$$

Since r_{ave} satisfies (A.8), we know using Proposition 1 and Theorem 1 that $\lambda_1\left(\bar{A}\right) \leq -\epsilon$. Consider the Lyapunov candidate $V(t) = 1/2x^Tx$:

$$\dot{V} = x^T\bar{A}x + x^T\left(-\bar{\mathcal{H}} + \mathcal{K}\right) \leq -\epsilon\|x\|^2 + x^T\mathcal{K}$$

The indefinite term $x^T\mathcal{K}$ is upper-bounded as

$$\begin{aligned} x^T\mathcal{K}(p,q) &= q^T\tilde{R}(I-P-Q)(\beta_1Ap+\beta_2Aq) \\ &\leq \|q\|\|\tilde{R}\|\|(I-P-Q)\|(\beta_1\|A\|\|p\| + \beta_2\|A\|\|q\|) \\ &\leq \|q\|\tilde{r}_{max}\lambda_1(A)(\beta_1\|p\| + \beta_2\|q\|) \\ &\leq \tilde{r}_{max}\lambda_1(A)\beta_2\|q\|(\|p\| + \|q\|) \\ &\leq \tilde{r}_{max}\lambda_1(A)\beta_2\|x\|(\|x\| + \|x\|) \\ &= 2\tilde{r}_{max}\lambda_1(A)\beta_2\|x\|^2 \end{aligned}$$

where to write the third inequality, we considered $\beta_1 < \beta_2$. Hence,

$$\dot{V} \leq -(\epsilon - 2\tilde{r}_{max}\lambda_1(A)\beta_2)\|x\|^2$$

Having $\tilde{r}_{max} < \epsilon/2\beta_2\lambda_1(A)$ renders $\dot{V}$ negative definite.

Appendix B. Mean field approximation of BOB model

To see how the N-intertwined model (1) is derived as a mean field approximation of the exact Markov process, let, for each node $i \in \{1,\dots,N\}$, $X_i : \{B, O\}$ be a random variable, and X_i^t the value of X_i at time t. The epidemic spread dynamics of BOB is then modeled as the following continuous-time Markov process:

$$\begin{aligned} &\Pr\left(X_i^{t+\Delta t} = O | X_i^t = B, \boldsymbol{X}^t\right) = \beta_1\Delta t Y_i^t + o(\Delta t) \\ &\Pr\left(X_i^{t+\Delta t} = B | X_i^t = O, \boldsymbol{X}^t\right) = \delta_1\Delta t + o(\Delta t) \end{aligned} \tag{B.1}$$

where $i \in \{1,\dots,N\}$, $Y_i^t \triangleq \sum_{j\in\mathcal{N}_i} a_{ij}1_{\{X_j^t=O\}}$, with $1_{\{\mathcal{X}\}}$ the indicator function. In (B.1), Pr(.) denotes probability, $\boldsymbol{X}^t \triangleq \{X_i^t, i = 1,\dots,N\}$ is the joint state of the network, and Δt is a time step. Now, the mean field approximation (1) is obtained as explained as follows. By taking expectation of (B.1), the exact Markovian dynamics of the system is obtained where the evolution of the marginal information of each state depends on the evolution of pairwise joint probability of combination of states that itself depends on the higher order joint probabilities and so forth; therefore, the size of the state space increases exponentially. The mean-field closure approximation estimates the marginal probabilities using only marginal information and thus prevents the explosion of the state-space. Using this mean field approximation procedure, it is possible to express the transition probabilities in terms of the corresponding expected values. Specifically, the term $1_{\{X_j^t=O\}}$ is replaced with $\mathrm{E}[1_{\{X_j^t=O\}}]$, where E[.] denotes the expected value. Then, using the fact that p_i and b_i are not independent, since $b_i + p_i = 1$, we obtain the N-intertwined Eq. (1).

Appendix C. Networks with small-world effects

To illustrate that our results remain unaffected with varying the network type and that they also well apply to networks with small-world effects (Newman, 2018), we examine the heterogeneous optimal incentive distribution for a Watts–Strogatz (WS) network with 1000 nodes. All other conditions are similar to those considered for Fig. 12, to minimize the effect of parameters other than the network type. We also admit an spectral radius $\lambda_1(A) = 14.3066$ for WS network, which was achieved with an average degree of 14 and rewiring probability 0.5 in a WS network with 1000 nodes. Hence, the spectral radius for WS network is near to that of ER network in Fig. 12 with $\lambda_1(A) = 14.9380$. The results are seen in Fig. C.14. A comparison of Figs. 12 and C.14 reveals that results are qualitatively unchanged.

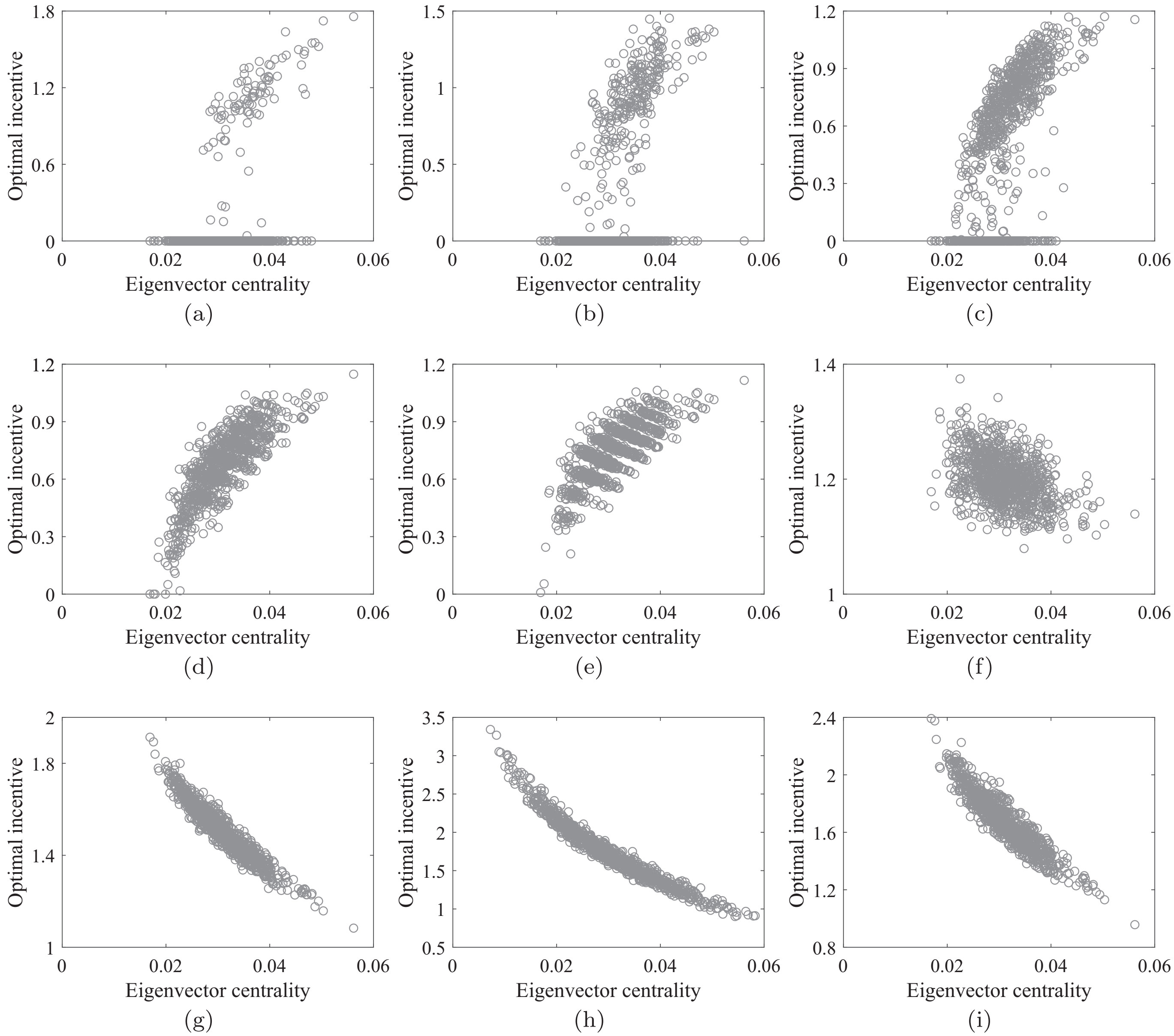

Fig. C14. Optimal incentives versus eigenvector centrality for a WS network of 1000 nodes and average degree 14 when (a) $\boldsymbol{c} = \mathbf{100}$, (b) $\boldsymbol{c} = \mathbf{250}$, (c) $\boldsymbol{c} = \mathbf{500}$, (d) $\boldsymbol{c} = \mathbf{675}$, (e) $\boldsymbol{c} = \mathbf{750}$, (f) $\boldsymbol{c} = \mathbf{1200}$, (g) $\boldsymbol{c} = \mathbf{1500}$, (h) $\boldsymbol{c} = \mathbf{2000}$, (i) the total incentive is not limited $(\boldsymbol{c} = \infty)$.

References

Ajorlou, A., & Jadbabaie, A. (2019). Sales-based rebate design. *Available at SSRN 3348692*.

Ajorlou, A., Jadbabaie, A., & Kakhbod, A. (2016). Dynamic pricing in social networks: The word-of-mouth effect. *Management Science, 64*(2), 971–979.

Ameri, M., Honka, E., & Xie, Y. (2019). Word of mouth, observed adoptions, and anime-watching decisions: The role of the personal vs. the community network. *Marketing Science*.

Antulov-Fantulin, N., Lančić, A., Štefančić, H., & Šikić, M. (2013). Fastsir algorithm: A fast algorithm for the simulation of the epidemic spread in large networks by using the susceptible–infected–recovered compartment model. *Information sciences, 239*, 226–240.

Arthur, D., Motwani, R., Sharma, A., & Xu, Y. (2009). Pricing strategies for viral marketing on social networks. In *Internet and network economics* (pp. 101–112).

Bampo, M., Ewing, M. T., Mather, D. R., Stewart, D., & Wallace, M. (2008). The effects of the social structure of digital networks on viral marketing performance. *Information systems research, 19*(3), 273–290.

Bapna, R., & Umyarov, A. (2015). Do your online friends make you pay? a randomized field experiment on peer influence in online social networks. *Management Science, 61*(8), 1902–1920.

Berger, J., & Milkman, K. (2010). Social transmission, emotion, and the virality of online content. *Wharton research paper, 106*, 1–52.

Biyalogorsky, E., Gerstner, E., & Libai, B. (2001). Customer referral management: Optimal reward programs. *Marketing Science, 20*(1), 82–95.

Bloch, F., & Quérou, N. (2013). Pricing in social networks. *Games and economic behavior, 80*, 243–261.

Boyd, S., Kim, S.-J., Vandenberghe, L., & Hassibi, A. (2007). A tutorial on geometric programming. *Optimization and engineering, 8*(1), 67.

Brunton, S. L., & Kutz, J. N. (2019). *Data-driven science and engineering: Machine learning, dynamical systems, and control*. Cambridge University Press.

Bullo, F. (2018). *LECTURES ON NETWORK SYSTEMS.*. CreateSpace.

Bullo, F. (2019). *Lectures on Network Systems* (1st). Kindle Direct Publishing. With contributions by J. Cortes, F. Dorfler, and S. Martinez

Candogan, O., Bimpikis, K., & Ozdaglar, A. (2012). Optimal pricing in networks with externalities. *Operations Research, 60*(4), 883–905.

Carroni, E., Pin, P., & Righi, S. (2019). Bring a friend! privately or publicly? *Management Science*.

Chen, W., Lu, P., Sun, X., Tang, B., Wang, Y., & Zhu, Z. A. (2011). Optimal pricing in social networks with incomplete information. In *International workshop on internet and network economics* (pp. 49–60). Springer.

Christophe, V., Wuyts, S., Dekimpe, M., Gijsbrechts, E., & Pieters, R. (2010). Opportunities and challenges in studying consumer networks. *The Connected Customer, S. Wuyts, MG Dekimpe, E. Gijsbrechts, and R. Pieters (eds.), London, Routledge*, 7–35.

Cohen, M. C., & Harsha, P. (2019). Designing price incentives in a network with social interactions. *Manufacturing & Service Operations Management*.

Domingos, P., & Richardson, M. (2001). Mining the network value of customers. In *Proceedings of the seventh acm sigkdd international conference on knowledge discovery and data mining* (pp. 57–66).
Fall, A., Iggidr, A., Sallet, G., & Tewa, J.-J. (2007). Epidemiological models and lyapunov functions. *Mathematical Modelling of Natural Phenomena, 2*(1), 62–83.
Farina, L., & Rinaldi, S. (2011). *Positive linear systems: theory and applications*. John Wiley.
Goel, S., Anderson, A., Hofman, J., & Watts, D. J. (2015). The structural virality of online diffusion. *Management Science, 62*(1), 180–196.
Hartline, J., Mirrokni, V., & Sundararajan, M. (2008). Optimal marketing strategies over social networks. In *Proceedings of the 17th international conference on world wide web* (pp. 189–198). ACM.
Hethcote, H. W. (2000). The mathematics of infectious diseases. *SIAM review, 42*(4), 599–653.
Hinz, O., Skiera, B., Barrot, C., & Becker, J. U. (2011). Seeding strategies for viral marketing: An empirical comparison. *Journal of Marketing, 75*(6), 55–71.
Hu, M., Milner, J., & Wu, J. (2015). Liking and following and the newsvendor: Operations and marketing policies under social influence. *Management Science, 62*(3), 867–879.
Hu, Z.-H., & Sheng, Z.-H. (2015). Disaster spread simulation and rescue time optimization in a resource network. *Information Sciences, 298*, 118–135.
Iyengar, S. S., & Lepper, M. R. (2000). When choice is demotivating: Can one desire too much of a good thing? *Journal of personality and social psychology, 79*(6), 995.
Kempe, D., Kleinberg, J., & Tardos, É. (2003). Maximizing the spread of influence through a social network. In *Proceedings of the ninth acm sigkdd international conference on knowledge discovery and data mining* (pp. 137–146).
Khalil, H. K. (2014). *Nonlinear control*. Pearson.
Khanafer, A., Başar, T., & Gharesifard, B. (2016). Stability of epidemic models over directed graphs: A positive systems approach. *Automatica, 74*, 126–134.
Kiss, I. Z., Miller, J. C., Simon, P. L., et al. (2017). *Mathematics of epidemics on networks*: 598. Springer.
Van der Lans, R., Van Bruggen, G., Eliashberg, J., & Wierenga, B. (2010). A viral branching model for predicting the spread of electronic word of mouth. *Marketing Science, 29*(2), 348–365.
Liao, H., Mariani, M. S., Medo, M., Zhang, Y.-C., & Zhou, M.-Y. (2017). Ranking in evolving complex networks. *Physics Reports, 689*, 1–54.
Lobel, I., Sadler, E., & Varshney, L. R. (2016). Customer referral incentives and social media. *Management Science, 63*(10), 3514–3529.
Lorch, L., De, A., Bhatt, S., Trouleau, W., Upadhyay, U., & Gomez-Rodriguez, M. (2018). Stochastic optimal control of epidemic processes in networks. *arXiv preprint arXiv:1810.13043*.
Mandel, A., & Venel, X. (2020). Dynamic competition over social networks. *European Journal of Operational Research, 280*(2), 597–608.
Mei, W., Mohagheghi, S., Zampieri, S., & Bullo, F. (2017). On the dynamics of deterministic epidemic propagation over networks. *Annual Reviews in Control, 44*, 116–128.
Meyners, J., Barrot, C., Becker, J. U., & Bodapati, A. V. (2017). Reward-scrounging in customer referral programs. *International Journal of Research in Marketing, 34*(2), 382–398.
Mieghem, P. V. (2011). The *N*-intertwined SIS epidemic network model. *Computing, 93*, 147??–169.
Nasirian, F., Pajouh, F. M., & Balasundaram, B. (2020). Detecting a most closeness–central clique in complex networks. *European Journal of Operational Research, 283*(2), 461–475.
Newman, M. (2018). *Networks* (2nd). Oxford University Press.
Nocedal, J., & Wright, S. (2006). *Numerical optimization*. Springer-Verlag New York.
Nowzari, C., Preciado, V. M., & Pappas, G. J. (2016). Analysis and control of epidemics: A survey of spreading processes on complex networks. *IEEE Control Systems Magazine, 36*(1), 26–46.
Ogura, M., & Preciado, V. M. (2018). Second-order moment-closure for tighter epidemic thresholds. *Systems & Control Letters, 113*, 59–64.
Pescher, C., Reichhart, P., & Spann, M. (2014). Consumer decision-making processes in mobile viral marketing campaigns. *Journal of interactive marketing, 28*(1), 43–54.
Preciado, V. M., Zargham, M., Enyioha, C., Jadbabaie, A., & Pappas, G. (2013). Optimal vaccine allocation to control epidemic outbreaks in arbitrary networks. In *52nd ieee conference on decision and control* (pp. 7486–7491). IEEE.
Preciado, V. M., Zargham, M., Enyioha, C., Jadbabaie, A., & Pappas, G. J. (2014). Optimal resource allocation for network protection against spreading processes. *IEEE Transactions on Control of Network Systems, 1*(1), 99–108.
Raghavan, S., & Zhang, R. (2019). A branch-and-cut approach for the weighted target set selection problem on social networks. *Informs Journal on Optimization*, ijoo–2019.
Sahneh, F., Chowdhury, F., Brase, G., & Scoglio, C. (2014). Individual-based information dissemination in multilayer epidemic modeling. *Mathematical Modelling of Natural Phenomena, 9*(2), 136–152.
Sahneh, F. D., & Scoglio, C. (2013). *May the best meme win!: New exploration of competitive epidemic spreading over arbitrary multi-layer networks*. arXiv preprint arXiv:1308.4880.
Sahneh, F. D., Scoglio, C., & Chowdhury, F. N. (2013a). Effect of coupling on the epidemic threshold in interconnected complex networks: A spectral analysis. In *2013 american control conference* (pp. 2307–2312). IEEE.
Sahneh, F. D., Scoglio, C., & Van Mieghem, P. (2013b). Generalized epidemic mean-field model for spreading processes over multilayer complex networks. *IEEE/ACM Transactions on Networking (TON), 21*(5), 1609–1620.
Sahneh, F. D., & Scoglio, C. M. (2012). Optimal information dissemination in epidemic networks. In *2012 ieee 51st ieee conference on decision and control (cdc)* (pp. 1657–1662). IEEE.
Sahneh, F. D., Vajdi, A., Shakeri, H., Fan, F., & Scoglio, C. (2017). Gemfsim: a stochastic simulator for the generalized epidemic modeling framework. *Journal of computational science, 22*, 36–44.
Shakeri, H., Sahneh, F. D., Scoglio, C., Poggi-Corradini, P., & Preciado, V. M. (2015). Optimal information dissemination strategy to promote preventive behaviors in multilayer epidemic networks. *Mathematical Biosciences and Engineering, 12*(3), 609–623.
Stewart, D., Ewing, M., & Mather, D. (2004). e-audience estimation: Modelling the spread of viral advertising using branching theory. In *Annual meeting, institute for operations research and the management sciences, denver, co* (pp. 24–27).
Tanınmış, K., Aras, N., & Altınel, I. (2019). Influence maximization with deactivation in social networks. *European Journal of Operational Research, 278*(1), 105–119.
Urena, R., Kou, G., Dong, Y., Chiclana, F., & Herrera-Viedma, E. (2019). A review on trust propagation and opinion dynamics in social networks and group decision making frameworks. *Information Sciences, 478*, 461–475.
Van Mieghem, P., Omic, J., & Kooij, R. (2009a). Virus spread in networks. *IEEE/ACM Transactions on Networking (TON), 17*(1), 1–14.
Van Mieghem, P., Omic, J., & Kooij, R. (2009b). Virus spread in networks. *IEEE/ACM Transactions on Networking (TON), 17*(1), 1–14.
Wang, Y., Chakrabarti, D., Wang, C., & Faloutsos, C. (2003). Epidemic spreading in real networks: An eigenvalue viewpoint. In *22nd international symposium on reliable distributed systems, 2003. proceedings.* (pp. 25–34). IEEE.
Watkins, N. J., Nowzari, C., & Pappas, G. J. (2017). Inference, prediction and control of networked epidemics. In *2017 american control conference (acc)* (pp. 5611–5616). IEEE.
Watkins, N. J., Nowzari, C., & Pappas, G. J. (2018). Robust economic model predictive control of continuous-time epidemic processes. *arXiv preprint arXiv:1707.00742*.
Watts, D. J., & Dodds, P. S. (2007). Influentials, networks, and public opinion formation. *Journal of consumer research, 34*(4), 441–458.
Xia, C., Wang, Z., Zheng, C., Guo, Q., Shi, Y., Dehmer, M., & Chen, Z. (2019). A new coupled disease-awareness spreading model with mass media on multiplex networks. *Information Sciences, 471*, 185–200.
Yang, L., Li, Z., & Giua, A. (2020). Containment of rumor spread in complex social networks. *Information Sciences, 506*, 113–130.
Yu, Z., Wang, C., Bu, J., Wang, X., Wu, Y., & Chen, C. (2015). Friend recommendation with content spread enhancement in social networks. *Information Sciences, 309*, 102–118.